HHS Public Access

Author manuscript

Biomed Pharmacother. Author manuscript; available in PMC 2023 October 01.

Published in final edited form as:

Biomed Pharmacother. 2023 October ; 166: 115399. doi:10.1016/j.biopha.2023.115399.

CFTR potentiator ivacaftor protects against noise-induced hair cell loss by increasing Nrf2 and reducing oxidative stress

Fan Wu[a,c,d,e,1], **Rui Hu**[a,b,d,1], **Xueping Huang**[a,c,d], **Jintao Lou**[a,c,d], **Ziyi Cai**[a,c,d], **Guisheng Chen**[a,c,d], **Wenji Zhao**[a,c,d], **Hao Xiong**[a,c,d], **Su-Hua Sha**[e,*], **Yiqing Zheng**[a,b,c,d,**]

[a]Department of Otolaryngology, Sun Yat-sen Memorial Hospital, Sun Yat-sen University, Guangzhou, Guangdong, China

[b]Shenshan Medical Center, Memorial Hospital of Sun Yat-sen University, Shanwei, Guangdong, China

[c]Guangdong Provincial Key Laboratory of Malignant Tumor Epigenetics and Gene Regulation, Sun Yat-sen Memorial Hospital, Sun Yat-sen University, Guangzhou, Guangdong, China

[d]Institute of Hearing and Speech-Language Science, Sun Yat-sen University, Guangzhou 510120, China

[e]Department of Pathology and Laboratory Medicine, The Medical University of South Carolina, Charleston, SC, USA

Abstract

Over-production of reactive oxygen species (ROS) in the inner ear can be triggered by a variety of pathological events identified in animal models after traumatic noise exposure. Our previous research found that inhibition of the AMP-activated protein kinase alpha subunit (AMPKα) protects against noise-induced cochlear hair cell loss and hearing loss by reducing ROS

*Correspondence to: Department of Pathology and Laboratory Medicine, Medical University of South Carolina, Walton Research Building, Room 403-E, 39 Sabin Street, Charleston, SC 29425, USA. shasu@musc.edu (S.-H. Sha). **Correspondence to: Department of Otolaryngology, Sun Yat-sen Memorial Hospital and Institute of Hearing and Speech-Language Science, Sun Yat-sen University, 107 West Yan Jiang Road, Guangzhou 510120, Guangdong Province, China. zhengyiq@mail.sysu.edu.cn (Y. Zheng).
[1]These authors contributed equally to this work.

Ethics approval and consent to participate

No human data or tissue were involved. Animal research protocol was approved by the Institutional Animal Care and Use Committee at Sun Yat-sen University (# 2022000647). Animal care was under the supervision of Laboratory Animal Management Center of Sun Yat-sen University.

CRediT authorship contribution statement

These authors contributed equally to this work. FW, RH, XH, JL, ZC, GC, and WZ, performed research; FW and HX analyzed data; FW, YZ, and SS wrote the manuscript. All authors have reviewed the contents of the manuscript, approve of its contents, and validate the accuracy of the data.

Declaration of Competing Interest

The authors declare that they have no competing interests.

Author disclosure statement

There are no conflicts of interest for any of the authors. The data contained in the manuscript have not been previously published, have not been submitted elsewhere, and will not be submitted elsewhere while under review. All authors have reviewed the contents of the manuscript, approve of its contents, and validate the accuracy of the data. There are no use of generative AI and AI-assisted technologies in the writing process.

Appendix A. Supporting information

Supplementary data associated with this article can be found in the online version at doi:10.1016/j.biopha.2023.115399.

accumulation. However, the molecular pathway through which AMPKα exerts its antioxidative effect is still unclear. In this study, we have investigated a potential target of AMPKα and ROS, cystic fibrosis transmembrane conductance regulator (CFTR), and the protective effect against noise-induced hair cell loss of an FDA-approved CFTR potentiator, ivacaftor, in FVB/NJ mice, mouse explant cultures, and HEI-OC1 cells. We found that noise exposure increases phosphorylation of CFTR at serine 737 (p-CFTR, S737), which reduces wildtype CFTR function, resulting in oxidative stress in cochlear sensory hair cells. Pretreatment with a single dose of ivacaftor maintains CFTR function by preventing noise-increased p-CFTR (S737). Furthermore, ivacaftor treatment increases nuclear factor E2-related factor 2 (Nrf2) expression, diminishes ROS formation, and attenuates noise-induced hair cell loss and hearing loss. Additionally, inhibition of noise-induced AMPKα activation by compound C also diminishes p-CFTR (S737) expression. In line with these in-vivo results, administration of hydrogen peroxide to cochlear explants or HEI-OC1 cells increases p-CFTR (S737) expression and induces sensory hair cell or HEI-OC1 cell damage, while application of ivacaftor halts these effects. Although ivacaftor increases Nrf2 expression and reduces ROS accumulation, cotreatment with ML385, an Nrf2 inhibitor, abolishes the protective effects of ivacaftor against hydrogen-peroxide-induced HEI-OC1 cell death. Our results indicate that noise-induced sensory hair cell damage is associated with p-CFTR. Ivacaftor has potential for treatment of noise-induced hearing loss by maintaining CFTR function and increasing Nrf2 expression for support of redox homeostasis in sensory hair cells.

Keywords

Noise-induced hearing loss; Activation of AMPKα; Reactive oxygen species; Cystic fibrosis transmembrane conductance; regulator ivacaftor; Nuclear factor E2-related factor 2

1. Introduction

Noise-induced hearing loss (NIHL) is one of the major causes of acquired hearing loss [1]. Prolonged exposure to high intensities of sound, such as that at industrial sites and music concerts, may result in loss of hair cells in the inner ear, which transduce sound vibrations into nerve signals. These sensory cells are highly vulnerable to various forms of inner ear insults, including noise trauma [2]. Since mammalian hair cells cannot be regenerated, their loss leads to irreversible hearing loss, reducing quality of life, increasing social isolation of the individual, and negatively impacting productivity and the economy [3]. Hearing aids can mitigate the detrimental effects of moderate hair cell loss but fail to restore good communication in cases of profound hearing loss or deafness [4]. Cochlear implants are used clinically for treatment of deafness but the outcomes depend highly on quantity and quality of surviving spiral ganglion neurons [5,6].

Protection of hair cells against traumatic insults has long been attempted, in both animal models and clinical trials. Antioxidant therapies have shown considerable promise in animals but translation to humans has had variable success. For example, in line with animal studies, a GPx1 mimetic, ebselen, showed a beneficial effect against noise-induced temporary hearing loss in a phase 2 clinical trial (ClinicalTrials.gov, number: NCT01444846) [7]. Contrary to animal studies, however, a dietary supplement of

antioxidants comprised of β-carotene, vitamins C and E, and magnesium failed to protect against noise-induced temporary hearing loss (ClinicalTrials.gov, number: NCT00808470) [8]. This may be partly due to the type and severity of the insults but also to the complexity of the response to traumatic noise which might include a variety of competing cell death and survival pathways [9,10]. An additional challenge is finding effective drug delivery routes to the inner ear whose blood-labyrinth barrier (BLB) can limit entry of therapeutics [11].

Despite these setbacks, oxidative stress in sensory hair cells is a well-documented sequela to traumatic noise exposure in animal models [12], triggered by calcium overload, transient ATP depletion, mitochondrial damage, or general disruption of the antioxidative system [13,14]. We have previously documented ROS accumulation in sensory hair cells and an increase in AMP-activated protein kinase α (AMPKα), as indicated by phosphorylation at its Thr172 site (p-AMPKα). Administration of the antioxidative compound N-acetylcysteine (NAC) or forskolin significantly reduced AMPKα activation and prevented noise-induced hair cell death [15]. Blocking AMPKα activation by compound C or small interfering RNA likewise attenuated noise-induced permanent-threshold--shift (PTS) or permanent hearing loss [16]. Furthermore, inhibition of enzymes upstream of AMPKα, such as liver kinase B 1 (LKB1), also known as serine/threonine kinase 11 (STK11), or calcium/calmodulin dependent protein kinase kinase beta (CaMKKβ), through siRNA- or adeno-associated-virus-mediated silencing also alleviated noise-induced damage in sensory hair cells [14,16]. However, the detailed mechanism by which the AMPKα pathway affects the fate of sensory hair cells in noise exposure requires further study.

Cystic fibrosis transmembrane conductance regulator (CFTR) protein is an ATP-binding cassette transporter associated with surface ion and fluid balance [17]. As an ion channel, CFTR is compromised in airway epithelia and other tissues of cystic fibrosis patients often due to mutated human CFTR chloride channels (mutation of F508del *CFTR*) [18]. However, wildtype CFTR dysfunction has been associated with accelerated degradation of the CFTR protein. Such wildtype CFTR deprivation in brain, heart, and lung tissues are associated with inflammation and oxidative stress [19]. CFTR activator ivacaftor is an FAD-approved potentiator of mutated human F508del *CFTR*. Unlike human F508del *CFTR,* ivacaftor does not potentiate mouse F508del *cftr* [20]. However, systemic ivacaftor treatment ameliorates hippocampal neuron atrophy in wildtype *cftr* in mice [19]. Furthermore, ivacaftor strongly promotes nuclear factor E2-related factor-2 (Nrf2) expression and nuclear translocation in mutated and wildtype human cystic fibrosis bronchial epithelial cells [21], which further promotes the translation of antioxidative gene elements, including NADPH oxidase 1 (*NOX1*), quinone oxidoreductase 1 *(NQO1),* superoxide dismutase 2 (*SOD2*), and heme oxygenase-1 (*HO1*) [22-24].

Wildtype CFTR is expressed on both inner and outer hair cells in the mouse cochlea, and its cellular docking is directed by the hair cell motor protein prestin [25]. AMPKα negatively regulates CFTR through phosphorylation of the CFTR S737 site in the R domain (p-CFTR S737), thus blocking its function as demonstrated in nasal ciliated epithelia cells [26]. However, the role of wildtype CFTR and a possible association with activation of AMPKα in NIHL are unknown. We, therefore, tested our hypothesis that wildtype CFTR regulates Nrf2 function in sensory hair cells after traumatic noise exposure. We postulated

that activation of wildtype CFTR by ivacaftor or the upstream regulator AMPKα promotes Nrf2 expression, maintaining oxidative homeostasis in sensory hair cells and ultimately alleviating NIHL. We first used an in-vivo FVB/NJ mouse model to assess p-CFTR (S737) and CFTR expression in the inner ear, with focus on damaged outer hair cells (OHCs) after noise exposure. We then used compound C or ivacaftor to manipulate CFTR activation and expression of Nrf2 in OHCs. Finally, we used an in-vitro organ culture model and inner ear cell line (HEI-OC1) to test the effect of ivacaftor against hydrogen-peroxide-induced cell death to probe the relationship between ROS formation and CFTR activation. To our knowledge, this is the first study clarifying the relationship between wildtype CFTR activation and NIHL. Our results may provide new potential molecular targets for prevention of NIHL.

2. Materials and methods

2.1. Animals

FVB/NJ breeder mice (stock #GDMLAC-211) at the age of 4 weeks were purchased from Guang Dong Medical Laboratory Animal Center (GDMLAC, China). FVB/NJ mice used for all experiments were bred in the animal facility of the Laboratory Animal Management Center of Sun Yat-sen University. All mice had free access to water and a regular mouse diet (#GDMLAC-260, GDMLAC, China) under a standard 12:12-h light-dark cycle with the room kept at approximately 22 °C and the background environmental sound levels maintained at approximately 50 dB sound pressure level (SPL). Animal research protocols were approved by the Institutional Animal Care and Use Committee at Sun Yat-sen University (# 2022000647). Animal care was under the supervision of Laboratory Animal Management Center of Sun Yat-sen University. In this study, baseline ABRs of all mice were measured 3 days prior to noise exposure. Mice were excluded from the study if their baseline auditory thresholds were above 40 dB SPL at any of the measured frequencies. Both sexes of male and female FVB/NJ mice at the age of 4 weeks were exposed to noise. Previous studies showed no significant difference in sensitivity to noise exposure between male and female FVB/NJ mice at the age of 4 weeks [14,27].

2.2. Drug administration via intraperitoneal injection

Both compound C (#HY-13418A, MedChemExpress) and ivacaftor (#HY-13017, MedChemExpress) were dissolved in dimethyl sulfoxide (DMSO, #D2650, Sigma-Aldrich) as stock solutions (30 mg/mL) and stored at − 20 °C. Previously, we found that 20 mg/kg compound C significantly attenuated NIHL; we used 20 mg/kg in these experiments [16]. Each animal received a total of three intraperitoneal (IP) injections of compound C as previously reported [16]. Three IP injections were administered 1 day before, 2 h before, and 1 h after noise exposure. The metabolic half-life of ivacaftor is approximately 12 h [28] and has been used at 5–10 mg/kg in prior studies [29,30]. We also used 5–10 mg/kg in our pilot experiments and found 10 mg/kg to reduce hearing loss. Thus, mice received an IP injection of ivacaftor at 10 mg/kg 2 h before noise exposure. Vehicle control mice received the same volume of DMSO.

2.3. Noise exposure

FVB mice at the age of 4 weeks in separate 10 × 10 × 10-cm cages were exposed to broadband noise (BBN: 2–20 kHz) at 108 dB SPL for 2 h as previously described [31]. Since this noise condition causes OHC loss and permanent threshold shifts, we refer to it as PTS-inducing noise (PTSN). Briefly, unrestrained mice were placed in a sound chamber equipped with a loudspeaker (#HG220–1, New Retone, China) driven by a power amplifier (#P9500S, Yamaha, Japan). Sound levels in the chamber were measured by a sound level meter throughout the chamber (#1200; Quest Technologies, USA). The background sound intensity of the environment surrounding the chamber was 65 dB SPL. The sound meter was calibrated following the manufacturer's instructions (Quest Technologies, USA). Control mice were kept within the same chamber in silence (with the loudspeaker off) for 2 h (Fig. 1D schematic illustrates the timeline of the in-vivo experiments).

2.4. Auditory brainstem response measurement

ABRs were measured at before and 2 weeks post noise exposure as previously described [16]. Briefly, mice were anesthetized by IP injection of ketamine (100 mg/kg) and xylazine (10 mg/kg) and then were placed in a sound-isolated booth. Body temperature was kept near 37 °C with a heating pad. Acoustic stimuli were delivered by a loudspeaker. Three subdermal electrodes were inserted at the vertex of the skull (active), mastoid region under the left ear, and mastoid region under the right ear (ground). ABRs were recorded at 8-, 16-, and 32-kHz frequencies in the left ear of each mouse using Tucker-Davis Technologies (TDT) System III hardware (Alachua, FL, USA). A total of 1024 responses were obtained and SigGen/Biosig software was used to present the stimuli and record responses. ABR wave II was used to determine thresholds for each frequency. Thresholds were determined by reducing the intensity in 10-dB increments until no organized responses were detected and assigned by an expert who was blinded to the treatment conditions.

2.5. Immunolabeling for cochlear surface preparations

We have followed a procedure as previously described [16]. Briefly, the temporal bones were carefully removed and perfused locally through the round window membrane with 4 % paraformaldehyde (PFA, #158127, Sigma-Aldrich), pH 7.4, and were kept in this fixative overnight at 4 °C. After decalcification with 4 % sodium EDTA solution (adjusted with HCl to pH 7.4) for 2 days at 4 °C, the cochleae were micro-dissected into three turns (apex, middle, and base) and adhered to 10-mm round coverslips (#260367, Microscopy Products for Science and Industry, USA) with cell-Tak (#354240, BD Biosciences, USA). The specimens were first permeabilized in 1 % Triton X-100 solution for 10 min and then blocked with 10 % normal goat serum for 30 min at room temperature, followed by incubation at 4 °C for 24 h with the following primary antibodies: rabbit polyclonal anti-p-CFTR (S737) (#AF8042, Affinity Biosciences, China), rabbit polyclonal anti-CFTR (#FNab01623, FineTest, China), mouse monoclonal anti-Nrf2 (#66501-Ig, Proteintech, China), and rabbit polyclonal anti-4-hydroxynonenal (#46545, Abcam, USA). The specimens were then incubated with Alexa-Fluor-594-conjugated (#8889 or #8890, Cell Signaling Technology, USA) or Alexa-Fluor-488-conjugated (32 or #4408, Cell Signaling Technology, USA) secondary antibodies at a concentration of 1:200 at 4 °C overnight,

followed by incubation with Alexa Fluor 633 phalloidin (#SB-YP0053, Share-bio, China) and DAPI (#HY-D0814, MedChemExpress) for 1 h at room temperature in darkness. Between each step, the samples were washed three times with PBS for 5 min each wash. For visualization of sensory hair cells, the specimens were incubated with polyclonal primary rabbit anti-myosin 7a antibody (#25–6790, Proteus Biosciences, USA) at 1:200 at 4 °C overnight followed by incubation with Alexa Fluor 594 secondary antibody at a concentration of 1:200 at 4 °C overnight in darkness and then were co-stained with Alexa Fluor 488 phalloidin (#8878, Cell Signaling Technology, USA) and DAPI for 1 h. After at least three final washes with PBS, all immunolabeling samples were mounted by adding 7 μL of mounting agent and sandwiched with another round coverslip and placed on a microscope slide. Finally, the edges were sealed with nail polish. Immunolabeled images were taken with a 63× magnification lens under identical Z-stack conditions using a Zeiss LSM 710 system. A detailed video protocol can be found in our previously published article [32].

2.6. Semi-quantification of the immunolabeling signals from outer hair cells of surface preparations

We adapted our standard protocol as in our prior experiments [16]. Briefly, based on phalloidin counterstaining, the regions of interest were outlined within individual OHCs. The targeted labeling in grayscale in OHCs was analyzed for semi-quantification. Immunolabeling for CFTR, p-CFTR (S737), Nrf2, and 4-hydroxynonenal (4-HNE) was semi-quantified from original images with 8-bit grayscale values using ImageJ software (Ver. 1.46r, National Institutes of Health, USA). The cochleae from each group were fixed and immunolabeled simultaneously with identical solutions and processed in parallel to reduce confounding factors. All cochlear surface preparations were counter-stained with phalloidin to illustrate OHC structure for confocal images. We analyzed the immunolabeling in the upper-basal OHC region (corresponding to 22–32-kHz frequencies) of surface preparations in 0.12-mm segments, each containing approximately 60 OHCs. The intensity of the background was subtracted, and the average grayscale intensity per cell was then calculated. The relative ratio was determined by normalizing to the control. There were no obvious differences between the apex and middle turn in all detected signals in the study.

2.7. Counts of hair cells

We used a standard protocol as in our prior experiments [16]. Briefly, images from the apex through the base of the Alexa-Fluor-488-phalloidin-stained preparations were captured using a 20× lens on a Zeiss microscope. The lengths of cochlear epithelia were measured and recorded in millimeters. OHCs were counted from the apex to the base along the entire length of the mouse cochlear spiral. The percentage of hair cell loss in each 0.5-mm length of epithelium was plotted as a function of the cochlear length as a cytocochleogram. The results were in agreement with prior literature [33].

2.8. Extraction of total cochlear protein

We adapted our standard protocol as previously described [16]. The cochleae were removed and dissected in 4 °C PBS containing a protease inhibitor cocktail (#11836170001, Roche, USA). To extract total protein, tissues from the cochleae of a single mouse (two ears) were

homogenized in ice-cold RIPA lysis buffer (#R0278, Sigma-Aldrich) containing phosphatase inhibitor cocktail III and Roche protease inhibitor using a glass tube and grinding pestle. Tissue debris was removed by centrifugation at 12,000×*g* at 4 °C for 15 min, and the supernatants were collected as the total protein fraction. The protein concentration was determined using a BCA protein assay kit (#P0012, Beyotime, China. The total protein samples were stored in a −80 °C freezer.

2.9. Organ cultures of cochlear explants

We adapted our standard methods for cochlear explant preparation as described in our previous study [34]. The explants were cultured in 1× basal Eagle's medium (#B9638, Sigma-Aldrich) containing 1 % bovine serum albumin (10GR100, Biofroxx, China) and 1 % insulin transferrin selenium (ITS, #51500056, Gibco, USA) at 37 °C in a humidified incubator with 5 % CO_2 before pretreatment with different agents for 12 h. The explants were then exposed to 10 mM hydrogen peroxide for 30 min. The subsequent fluorescence staining was done as per the methods described above.

2.10. Cell immunofluorescence staining assay

The mouse inner ear cell line HEI-OC1 was kindly provided by Dr. F. Kalinec at UCLA Health. Following the protocol as previously reported [35], HEI-OC1 cells were cultured in high-glucose Dulbecco's modified Eagle's medium (DMEM, #11965092, Gibco, USA) containing 10 % fetal bovine serum (FBS, #04–001–1ACS, Biological Industries, USA) under humidified atmosphere with 10 % CO_2 at 33 °C. Before immunofluorescence staining, HEI-OC1 cells were lifted with 0.25 % trypsin-EDTA (#25200056, Gibco, USA) and seeded on 10-mm round glass slides at a density of 3000 cells/slide. Based on our experimental design, HEI-OC1 cells were pretreated with 5 μM ivacaftor, 5 μM compound C or the same volume of DMSO for 12 h before exposure to 10 mM hydrogen peroxide for 15 min. Then the cell slides were fixed with 4 % PFA at room temperature for 1 h. The subsequent procedures were similar to the staining methods for the cochlear surface preparations described above.

2.11. Annexin V/PI assay

The annexin V/PI assay was performed following an online protocol [36]. Briefly, a FITC-Annexin V/PI Apoptosis Kit (#E-CK-A211, Elab Bioscience, China) was used to assess the hydrogen-peroxide-induced apoptosis of HEI-OC1 cells in accordance with the manufacturer's instructions. Briefly, HEI-OC1 cells were incubated in 6-well plates with DMEM supplemented with 10 % FBS medium. After pretreatment with 10 μM ivacaftor or vehicle control (DMSO) for 12 h, cells were exposed to 10 mM hydrogen peroxide for 15 min. Then the cells were gently suspended in binding buffer and incubated in the dark at room temperature for 15 min with 5 μL of Annexin V-FITC (fluorescein isothiocyanate) and 5 μL of PI (propidium iodide). The Annexin V-FITC- and PI-labeled cells were analyzed using a flow cytometer (BD Biosciences, USA).

2.12. Cell vitality assay

Cultured HEI-OC1 cells were seeded at a density of 5000 cells/well in a 96-well plate in triplicate. After attachment, the cells were treated with gradient doses of ML385 (#HY-100523, MedChemExpress) from 2.5 to 10 μM for 12 h. Then the cells were incubated for 2 h with the Cell Counting Kit 8 (CCK-8) reagent (100 μL/mL medium) (#K1018, APEx-BIO, China). The absorbance was determined at 490 nm using a microplate reader (BioTek Instruments, USA).

2.13. Western blot analysis

Cells from different groups were homogenized in RIPA buffer (#V900854, Sigma-Aldrich) containing 1 mM PMSF (#329-98-6, Roche, USA), protease inhibitor cocktail (#11836170001, Roche, USA), and phosphatase inhibitor cocktail (#P0044, Sigma-Aldrich) on ice for 30 min. The protein concentration was determined using a BCA protein assay kit (#P0012, Beyotime, China). Protein samples (30 μg, either from cochleae or HEI-OC1 cells) were separated by SDS-PAGE. After electrophoresis, the proteins were transferred onto a PVDF membrane (#IPVH00005, Millipore, USA) and blocked with a 5 % solution of BSA in PBS-0.1 % Tween 20 (PBS-T). The membranes were incubated with rabbit polyclonal anti-p-CFTR (S737) (1:1000, #AF8042, Affinity Biosciences, China), rabbit polyclonal anti-CFTR (1:1000, #FNab01623, FineTest, China), and mouse monoclonal anti-Nrf2 (1:1000, #66501-Ig, Proteintech, China) at 4 °C overnight and then were washed three times (10 min each) with PBS-T buffer. Next, the membranes were incubated with the appropriate secondary antibody at a concentration of 1:2500 for 1 h at room temperature. Following extensive washing of the membranes, the immunoblot bands were visualized by ECL Western Blotting Substrate (#34577, Thermo Scientific, USA). GAPDH (1:3000, #5174, Cell Signaling Technology, USA) was used as a sample loading control. Band images were captured using the Bio-Rad Gel Doc XR documentation system (Bio-Rad Laboratories, USA) and were analyzed using ImageJ software (Ver. 1.46r, National Institutes of Health, USA). First, the background staining density for each band was subtracted from the band density. Next, the probing protein to GAPDH ratio was calculated from the band densities run on the same gel to normalize for differences in protein loading. Finally, the difference in the ratio of the control and experimental bands was tested for statistical significance.

2.14. Dichlorodihydrofluorescein diacetate (DCFH-DA) assay

We followed a protocol from a reported method [37]. Briefly, after pretreatment with ivacaftor or DMSO for 12 h, HEI-OC1 cells were exposed to 10 mM hydrogen peroxide for 15 min. Then DCFH-DA probe was diluted in normal HEI-OC1 culture medium to 0.1 %, and HEI-CO1 cells were incubated with this medium at 37 °C in a humidified incubator for 1 h. Cells were washed 3 times with PBS and collected by 0.25 % trypsin-EDTA digestion. Then the cells were gently suspended in PBS, and ROS levels were measured using a flow cytometer (BD Biosciences). All the flow cytometry had over 3 independent runs.

2.15. Statistical analyses

Data were analyzed using SYSTAT 8.0 and GraphPad 5.0 software for Windows. Biological sample sizes were determined based on the variability of measurements and the magnitude

of the differences between groups, as well as experience from our previous studies, with stringent assessments of differences. Differences with multiple comparisons were evaluated by one-way ANOVA with multiple comparisons. Differences for single-pair comparisons were analyzed using two-tailed unpaired Student's *t* tests. Data for relative ratios of single-pair comparisons were analyzed with one-sample *t* tests. A p value < 0.05 was considered statistically significant. Data are presented as the means ± SD. Sample sizes are indicated for each figure.

3. Results

3.1. Noise-induced activation of AMPKα negatively regulates CFTR in sensory hair cells via increases in p-CFTR (S737)

First, we assessed whether PTS-inducing noise exposure resulted in an alteration of the phosphorylation of CFTR (S737) in OHCs. Immunolabeling for p-CFTR (S737) was high in the cytosol and nuclei of OHCs examined 3 h after noise exposure (Fig. 1A, panel: DMSO + PTS). The noise-induced increases were 5-fold in the cytosol ($p < 0.001$) and 4-fold in nuclei ($p < 0.001$). Since we had previously reported that noise exposure activates AMPKα, we then treated mice with the AMPKα inhibitor compound C. Noise-increased immunolabeling for p-CFTR (S737) in both the cytosol and nuclei of OHCs (Fig. 1A, panel: compound C + PTS) was significantly diminished (cytosol: $p = 0.029$, nuclei: $p < 0.001$) (Fig. 1B-C). In contrast, vehicle control with DMSO or compound C alone without noise exposure showed only weak immunolabeling for p-CFTR (S737) (Fig. 1A, panel: DMSO or compound C). These results suggest that activation of AMPKα increases p-CFTR (S737) in OHCs after noise exposure, which subsequently inhibits CFTR function.

3.2. Treatment with CFTR potentiator ivacaftor prevents noise-induced increases of p-CFTR (S737) and decreases of total CFTR in OHCs

Since ivacaftor is a CFTR potentiator, we used it to manipulate CFTR and p-CFTR (S737) in OHCs after noise exposure that causes PTS. Based on a report in the literature [38], we first tested doses of ivacaftor in our pilot experiments on mice from 5 mg/kg to 10 mg/kg by a single IP injection. The animals tolerated the treatment well, maintaining healthy-appearing fur and were without losses of auditory sensitivity or bodyweight during the following two weeks. In cochlear wholemount preparations, immunolabeling for CFTR (red) in the cytosol and nuclei of OHCs in the basal turn was weak, while p-CFTR (S737, green) was strong 3 h after noise exposure (Fig. 2A). Both the reduction of CFTR (cytosol: $p = 0.001$, nuclei: $p = 0.003$) and the enhancement of p-CFTR (S737) (cytosol: $p = 0.009$, nuclei: $p = 0.002$) were significant in OHCs (Fig. 2B-E). Treatment with a single dose of 10 mg/kg ivacaftor 2 h before PTS-noise exposure significantly prevented the noise-induced decrease in CFTR (cytosol: $p = 0.003$, nuclei: $p = 0.032$) and the increase in p-CFTR (S737) (cytosol: $p = 0.039$, nuclei: $p = 0.003$) in OHCs (Fig. 2B-E). Additionally, immunoblots using total cochlear homogenates (Fig. 2F) showed a reduced CFTR band at 160 kDa (20 % reduction; Fig. 2G, $p = 0.0056$) and a single, more intense p-CFTR (S737) band (3-fold increase; $p = 0.0027$) 3 h after PTS exposure. Confirming this analysis, the ratio of p-CFTR (S737) to CFTR increased 4-fold ($p = 0.0017$) (Fig. 2G-I). These results indicate that noise exposure increases p-CFTR (S737) levels, decreases total CFTR protein levels

and compromises CFTR function. Pretreatment with ivacaftor prevented these noise-induced effects in cochlear cells, including OHCs.

3.3. Treatment with ivacaftor increases Nrf2 and prevents noise-induced overproduction of reactive oxygen species in sensory hair cells

We next assessed whether pretreatment with ivacaftor mediates noise-induced oxidative stress in OHCs by analyzing Nrf2, which can be modulated by CFTR [21]. Immunolabeling for Nrf2 mildly increased in OHC cytosol and nuclei 3 h after noise exposure compared to vehicle controls without noise exposure (Fig. 3A, panels: DMSO + PTS vs. DMSO; Fig. 3B-C: cytosol: $p = 0.039$, nuclei: $p = 0.019$). Pretreatment with ivacaftor 2 h before noise exposure caused a robust 2-fold increase of Nrf2 immunolabeling in OHCs (Fig. 3A, panel: IVA + PTS; Fig. 3B-C: cytosol: $p = 0.005$, nuclei: $p = 0.001$). As a measure of oxidative stress, we assessed lipid peroxidation products 4-HNE with or without ivacaftor pretreatment 3 h after noise exposure. Consistent with our previous study [15], immunolabeling for 4-HNE (Fig. 4A) in both the cytosol and nuclei of OHCs was higher after noise exposure compared to controls without noise (cytosol: $p = 0.004$, nuclei: $p = 0.012$). In contrast, pretreatment with ivacaftor almost completely prevented noise-increased 4-HNE labeling in OHCs (Fig. 4B-C; cytosol: $p = 0.011$, nuclei: $p = 0.037$). These results suggest that pretreatment with ivacaftor may maintain ROS homeostasis in sensory hair cells after noise exposure.

3.4. Treatment with ivacaftor attenuates noise-induced loss of outer hair cell and auditory thresholds

We next extended our studies by evaluating loss of hair cells and auditory thresholds in FVB/NJ mice in vivo. In pilot experiments, we had determined that exposure to 108 dB for 2 h resulted in permanent hearing loss with an approximately 60-dB auditory threshold shift at all tested frequencies (8, 16, and 32 kHz), assessed 14 days after the exposure. We then tested two doses (5 mg/kg and 10 mg/kg) of ivacaftor in a single IP injection for attenuation of NIHL in these pilots based on a report [38]. We chose pretreatment with ivacaftor at 10 mg/kg for better attenuation of NIHL. Ivacaftor significantly attenuated noise-induced threshold shifts, illustrated by ABR waveforms at 32 kHz (Fig. 5A). The average reduction of threshold shifts was about 20–25 dB at 8 ($p < 0.001$), 16 ($p < 0.001$), and 32 kHz ($p < 0.001$) (Fig. 5B). After final ABR measurements, we counted hair cells along the cochlear spiral. In agreement with our previous experiments, this noise condition only resulted in OHC loss following a base-to-apex gradient with cells in the base of the cochlea being most vulnerable (Fig. 5C). Noise induced 90 % loss of OHCs in the hook region (5.0–5.5 mm from the apex), 40 % loss in the lower basal turn (4.5 mm from the apex), and about 20 % in the middle of the basal turn (4.0 mm from the apex). Treatment with ivacaftor significantly reduced OHC loss ($F_{1,7} = 37.57$, $p = 0.0001$). Further analysis showed that the loss of OHCs was significantly reduced at 3–5.5 mm from the apex (except at 3 mm where $p = 0.011$, $p < 0.001$ from 3.5 to 5.5 mm) (Fig. D).

3.5. Ivacaftor reduces hydrogen-peroxide-induced hair cell damage in organotypic explant cultures

We applied hydrogen peroxide (30 min) with or without ivacaftor pretreatment to a postnatal day 3 (p3) cochlear explant culture model to assess a potential link between ROS formation with CFTR activity. There was no positive labeling for p-CFTR (S737) in explants with DMSO or ivacaftor alone without exposure to hydrogen peroxide (Fig. 6A). However, hydrogen peroxide induced dense labeling in OHCs (Fig. 6A, panel: DMSO + H_2O_2) to a 3-fold increase over controls ($p < 0.001$). Pretreatment with ivacaftor for 12 h before hydrogen peroxide application almost completely blocked p-CFTR (S737) labeling (Fig. 6A, panel: IVA + H_2O_2; $p < 0.001$). These results support the notion that ROS contribute to CFTR inhibition via increasing p-CFTR (S737) and that pre-administration of ivacaftor abolishes this deleterious effect.

Next, we probed hair cell death by TUNEL staining and co-labeling with the hair cell marker myosin-7a. Application of DMSO or ivacaftor alone did not induce apoptosis in hair cells and there was no hair cell loss (Fig. 6C-E). In contrast, exposure of explants to 10 mM hydrogen peroxide for 30 min significantly increased TUNEL-positive hair cells ($p < 0.001$) and decreased myosin-7a-labeled hair cells ($p < 0.001$), indicating significant hair cell loss (Fig. 6C-E). Pretreatment with ivacaftor reduced the number of TUNEL-positive cells and prevented hair cell loss ($p < 0.001$, Fig. 6C-E). These results are consistent with our in-vivo *data,* demonstrating that the protective effect of ivacaftor is mediated, at least in part, by inhibition of oxidative stress.

3.6. Compound C or ivacaftor diminishes hydrogen-peroxide-increased p-CFTR (S737) expression in an inner ear cell line

To further test a causative relationship between CFTR activation and oxidative stress, we exposed the HEI-OC1 inner ear cell line to hydrogen peroxide. In line with the above in-vivo and explant experiments, exposure to 10 mM hydrogen peroxide for 15 min produced strong p-CFTR (S737) band densities at 160 kDa (Fig. 7A) on Western blots (2-fold increase over controls; $p = 0.002$). Since compound C and ivacaftor are both shown to inhibit PTS-noise-increased p-CFTR (S737) in OHCs, we pretreated the HEI-OC1 cells with 5 μM compound C for 12 h prior to the application of hydrogen peroxide. Immunoblots revealed that the hydrogen-peroxide-induced p-CFTR (S737) band was nearly completely abolished by pretreatment with compound C (Fig. 7A-B; $p = 0.007$).

We then detailed the effects of hydrogen peroxide and ivacaftor on both CFTR and p-CFTR at the cellular level. Ivacaftor alone or the vehicle DMSO did not change total CFTR or p-CFTR (S737) labeling (Fig. 8A) compared to untreated controls. Exposure of HEI-OC1 cells to 10 mM hydrogen peroxide for 15 min showed the expected enhancement of the p-CFTR (S737) labeling ($p = 0.016$) and a significant reduction of CFTR ($p = 0.012$; Fig. 8A-C). p-CFTR (S737) labeling was strong in the cytosol and cell membrane (Fig. 8A, enlarged). Treatment with 5 μM ivacaftor for 12 h prior to exposure to hydrogen peroxide increased total CFTR ($p = 0.004$) and reduced p-CFTR (S737) labeling to near baseline levels ($p = 0.037$; Fig. 8A-C).

Confirming the results from immunolabeling studies, additional immunoblotting experiments showed no obvious changes in CFTR or p-CFTR (S737) bands in cells treated with DMSO- or ivacaftor-alone (Fig. 8D). After exposure to hydrogen peroxide, decreased CFTR ($p = 0.002$) and increased p-CFTR (S737) ($p = 0.014$) bands were detected in the 160-kDa region, and these effects were reversed by pretreatment with ivacaftor (CFTR: $p = 0.021$, p-CFTR: $p = 0.031$; Fig. 8D). Overall, the ratio of p-CFTR to CFTR increased 6-fold after hydrogen peroxide stimulation ($p = 0.002$) and this increase was significantly inhibited by pretreatment with ivacaftor ($p = 0.005$, Fig. 8E-G). These results further support the notion that activation of AMPKα negatively regulates CFTR function.

3.7. Ivacaftor improves cellular antioxidant status by an increase in Nrf2 expression and decrease in ROS formation in HEI-OC1 cells

The above in-vivo results suggested that treatment with ivacaftor maintained oxidative balance in OHCs after noise exposure. We then employed HEI-OC1 cells to test whether ivacaftor application also increased Nrf2 and decreased ROS formation after exposure to hydrogen peroxide. Ivacaftor alone or exposure to hydrogen peroxide weakly increased Nrf2 labeling compared to DMSO alone (IVA alone: $p = 0.049$, DMSO + H_2O_2: $p = 0.013$, Fig. 9 A-B). However, when the cells were pretreated with ivacaftor and then exposed to hydrogen peroxide, strong immunolabeling for Nrf2 was detected (IVA + H_2O_2; $p = 0.002$, Fig. 9 A-B). Furthermore, immunoblotting results confirmed a roughly 70 % increase in Nrf2 levels after ivacaftor alone ($p = 0.003$), a 50 % increase after hydrogen peroxide stimulation ($p = 0.04$), and further increased Nrf2 levels to more than double after combined application of ivacaftor and hydrogen peroxide treatment ($p = 0.001$) (Fig. 9D-E). In agreement with the preceding results, 4-HNE immunolabeling was strong in hydrogen-peroxide-exposed cells ($p = 0.001$) compared to DMSO- or ivacaftor-treated groups, indicating antioxidative stress of the cells. Pretreatment with ivacaftor diminished hydrogen-peroxide-enhanced 4-HNE labeling significantly ($p = 0.001$). Finally, we used a DCFH-DA probe to detect ROS accumulation in HEI-OC1 cells. After hydrogen peroxide exposure, strong green fluorescence was detected, with a significantly higher percentage of flow-cytometry-positive cells, analyzed as Geo mean levels ($p < 0.001$). This oxidative effect was almost completely abolished by ivacaftor pretreatment ($p < 0.001$, Fig. 9F-G).

3.8. Ivacaftor reduces ROS damage in HEI-OC1 cells in an Nrf2-dependent manner

Finally, we tried to verify whether the protective effect of ivacaftor against ROS-induced damage in HEI-OC1 cells occurred via Nrf2. ML385 is a well-studied specific Nrf2 inhibitor that suppresses Nrf2 expression [39,40]. We first used Western blots to quantify protein levels of Nrf2 in cells treated with concentrations of ML385 ranging from 2.5 μM to 10 μM. Administration of ML385 at 5 μM ($p = 0.018$) or 10 μM ($p = 0.002$) for 12 h markedly reduced Nrf2 levels (Fig. 10A-B), without loss of cell viability as measured by the CCK-8 assay (Fig. 10C). Treatment with ML385 alone thus had no obvious cytotoxicity. We continued with the lower dose of 5 μM ML385 since there was no significant difference between 5 μM and 10 μM in suppression of Nrf2 levels. HEI-OC1 cells were pretreated either with 5 μM ivacaftor alone or with ivacaftor and 5 μM ML385 for 12 h and then exposed to 10 mM hydrogen peroxide for 15 min. The control group was treated with the same dose of DMSO with no hydrogen peroxide stimulation. The

findings agreed with previous data, showing that exposure to hydrogen peroxide increases Nrf2 levels ($p = 0.007$) which were further increased by pretreatment with ivacaftor ($p = 0.015$) per Western blotting assessment (Fig. 10D-E). HEI-OC1 cells co-treated with ML385 showed a complete block of the ivacaftor-increased Nrf2 expression ($p < 0.001$) after hydrogen peroxide exposure (Fig. 10D-E). Concomitantly, apoptosis was detected by cleaved caspase-3 immunoblotting and Annexin V/PI apoptosis flow cytometry assays. The level of cleaved caspase-3 significantly increased after hydrogen peroxide stimulation ($p = 0.016$) and was reduced to normal control levels by ivacaftor pretreatment ($p = 0.017$). Importantly, the ability of ivacaftor to prevent the increase of cleaved caspase-3 was completely reversed by pre-treatment with ML385 ($p = 0.003$) (Fig. 10D, F). Annexin V/PI flow cytometry analysis found an incidence of hydrogen-peroxide-induced cellular apoptosis of approximately 30 % ($p = 0.004$) which was significantly reduced by pretreatment with ivacaftor ($p = 0.023$). However, this protective effect by ivacaftor was completely abolished by ML385 co-administration ($p = 0.003$) (Fig. 10G-H). These results indicate that the protective effect of ivacaftor against hydrogen peroxide damage is dependent upon increasing Nrf2 expression. Inhibition of Nrf2 expression by ML385 is sufficient to abolish ivacaftor's protective effect against hydrogen-peroxide-induced cell death.

4. Discussion

The salient results of this study are that traumatic noise exposure increases p-CFTR (S737) in sensory hair cells triggered by activation of AMPKα and accumulation of ROS. Activation of AMPKα inhibits CFTR activity via phosphorylation of CFTR at S737, indicated by the action of compound C, which inhibits AMPKα activation and effectively prevents noise-increased p-CFTR (S737). Accumulation of ROS is also associated with increased p-CFTR (S737) as indicated by the effect of the CFTR potentiator ivacaftor, which reduces noise-induced hair cell loss and hearing loss by mediating Nrf2 expression and maintaining oxidative homeostasis. These in-vivo results are supported by supplementary evidence, such as findings of hair cell death in explant cultures via suppression of Nrf2 expression and activation of caspase 3 after the administration of hydrogen peroxide. Likewise, administration of the specific Nrf2 inhibitor ML385 abolishes the protective effect of ivacaftor against hydrogen-peroxide-induced death of HEI-OC1 cells. To the best of our knowledge, this is the first demonstration of a potential regulation of CFTR by AMPKα activation and ROS accumulation after noise exposure, suggesting that hair cell loss and NIHL are mediated by CFTR. Ivacaftor is a compelling potential novel therapeutic agent as it attenuates NIHL with a single dose.

4.1. Noise-induced activation of AMPKα negatively regulates CFTR in sensory hair cells and treatment with the CFTR potentiator ivacaftor attenuates NIHL via increased Nrf2

CFTR is regulated by multiple kinase systems. AMPKα-activation-mediated CFTR inhibition by increasing p-CFTR (S737) is one of them [26,41]. Our results show that noise increases p-CFTR (S737) levels in the inner ear, including the cytosol and nuclei of OHCs in mice, while total CFTR expression decreases. Previously, we found that noise exposure significantly activates AMPKα (T172) in hair cells and that blockade of AMPKα activation, either by the specific inhibitor compound C or by silencing RNA, protects against NIHL

[16]. In agreement with the concept of activation of AMPKα negatively regulating CFTR partly via p-CFTR (S737) [26,41], our current study shows that noise-induced increases in p-CFTR (S737) in hair cells are significantly inhibited by compound C treatment.

Oxidative stress is a key event in NIHL [15,42-46]. Suppression of AMPKα activation profoundly reduces ROS levels in hair cells [15]. Meanwhile CFTR mediates cellular redox status [21] and is expressed in sensory hair cells [25]. Therefore, we have further addressed whether manipulation of CFTR expression contributes to noise-induced sensory hair cell loss and NIHL using the CFTR potentiator ivacaftor, as it rescues from Nrf2 dysfunction, increases Nrf2 expression in non-cystic fibrosis airway epithelia [21], and promotes the antioxidant transcription process [47]. Consistent with previous research [48], Nrf2 expression is slightly increased when measured 3 h after noise exposure, indicating a response of the cellular defense system. However, this mild increase in Nrf2 is not sufficient to reduce ROS formation, as assessed by 4-HNE levels at that time, in line with our previous reports [15,49,50]. Upon pretreatment with a single dose of ivacaftor, Nrf2 expression is further enhanced to double that of the noise exposure group, whereas noise-induced ROS accumulation indicated by 4-HNE immunolabeling in OHCs is significantly reduced. Furthermore, noise-induced OHC loss and hearing loss are also significantly attenuated. These results are aligned with the notion that CFTR inhibition causes a rapid increase in ROS levels [51]. They are also consistent with reports showing Nrf2 knockout mice are sensitive to noise exposure [52] and reveal Nrf2 as an effective target for prevention of NIHL.

4.2. Accumulation of ROS inhibits CFTR function, resulting in suppression of Nrf2, which leads to disruption of redox homeostasis and cell death

Our results using hydrogen peroxide on explant cultures or HEI-OC1 cells further support the association of AMPKα activation and the disruption of cellular redox homeostasis leading to cell death. Analogue to traumatic noise exposure causing sensory hair cell loss in vivo, exposure of explants or HEI-OC1 cells to hydrogen peroxide results in hair cell loss and OC1 cell death, respectively. Along with our in-vivo results, application of hydrogen peroxide decreases CFTR expression and increases p-CFTR (S737). These results indicate that the level of total CFTR protein is regulated directly or indirectly by ROS stimulation. Such results are consistent with a previous study showing that hydrogen peroxide diminishes CFTR expression in smooth muscle cells [53]. However, we have observed different localization of p-CFTR (S737) between OHCs after noise exposure and HEI-OC1 cells after hydrogen peroxide administration. In OHCs, noise induces increased p-CFTR (S737) in both the cytosol and nuclei, while in HEI-OC1 cells, hydrogen peroxide induces increased p-CFTR (S737) in the cytosol and cell membrane. This discrepancy might be due to the cell type as the HEI-OC1 cell line was developed from the postnatal organ of Corti of the immortomouse [54], harbors the simian virus 40 (SV40) large tumor antigen [55], and was cultured in the proliferation phase. The responses in HEI-OC1 cells might vary from responses in vivo, as we previously found the absence of cell death in the HEI-OC1 cells after aminoglycoside antibiotic (gentamicin) exposure [56].

Nevertheless, our in-vitro results show a similar phenomenon in which the CFTR activator ivacaftor increases Nrf2 expression and reduces ROS formation after hydrogen peroxide stimulation. Overall, these results provide important clues that the protective effect of ivacaftor is associated with Nrf2 expression. To prove this dependency, we have performed an Nrf2 inhibition experiment in HEI-OC1 cells. ML385 is a specific Nrf2 inhibitor that can reduce Nrf2 expression and its nuclear translocation [57]. We first found that inhibition of Nrf2 is dose-dependent in HEI-OC1 cells and there was no significant change in cell viability after treatment with 5 μM of ML385 for 12 h. This is consistent with previous studies [58,59]. Next, our immunoblot and annexin V/PI apoptotic flow cytometry data with ML385 cotreatment emphasize that the protective effect of ivacaftor against hydrogen peroxide stimulation in HEI-OC1 cells is dependent on Nrf2 expression.

In summary, our results first clarify the potential of CFTR as a new therapeutic target to prevent NIHL. The protective effect of maintaining CFTR to alleviate NIHL involves enhancement of Nrf2 expression and nuclear translocation, resulting in reduction of ROS accumulation in sensory hair cells. Moreover, CFTR activity is negatively regulated by activation of AMPKα in sensory hair cells after noise exposure. The results support our working hypothesis that noise exposure activates AMPKα and increases ROS formation. These sequelae in turn inhibit CFTR by increasing p-CFTR (S737) in OHCs. Treatment with ivacaftor diminishes noise-increased p-CFTR (S737) and increases Nrf2 expression, thus protects against noise-induced outer hair cell loss and hearing loss via inhibition of ROS damage (Fig. 11). Our results from this study may provide an impetus for drug development against NIHL as ivacaftor is an FAD-approved drug to treat certain types of cystic fibrosis. Furthermore, since oxidative stress has been involved in other forms of acquired hearing loss, such as ototoxic-drug- and age-related hearing loss, our results may also shed light on mechanisms for prevention of acquired hearing loss more generally.

Supplementary Material

Refer to Web version on PubMed Central for supplementary material.

Acknowledgements

We thank Dr. Jochen Schacht for his valuable comments on the manuscript and Andra Talaska for proofreading of the manuscript.

Funding

The research project described was supported by grants 2023M734004 from Postdoctoral Research Foundation of China (PI: F. Wu), 82201277 (PI: F. Wu), 82171134 (PI: H. Xiong), 82171138 (PI: Y. Zheng) from National Natural Science Foundation of China, and R01 DC009222 (PI: S-H. Sha) from the National Institute on Deafness and Other Communication Disorders, National Institutes of Health, USA.

Data Availability

Data will be made available on request.

Abbreviations:

4-HNE	4-hydroxynonenal

AMPKα	AMP-activated protein kinase alpha subunit
BLB	blood-labyrinth barrier
CaMKKβ	calcium/calmodulin dependent protein kinase kinase beta
CF	cystic fibrosis
CFTR	cystic fibrosis transmembrane conductance regulator
HEI-OC1 cells	inner-ear-derived cell line
HO1	heme oxygenase-1
IP	intraperitoneal
LKB1/STK11	liver kinase B 1/serine/threonine kinase 11
NAC	N-acetylcysteine
NIHL	noise-induced hearing loss
NOX1	NADPH oxidase 1
NQO1	quinone oxidoreductase 1
Nrf2	nuclear factor E2-related factor 2
OHCs	outer hair cells
p-CFTR S737	CFTR phosphorylated at serine 737 in the R domain
PTS	permanent threshold shift
PTSN	permanent threshold shift noise, specifically, broadband noise (BBN, 2–20 kHz) exposure for 2 h at 108 dB SPL inducing permanent threshold shifts in FVB/NJ mice
ROS	reactive oxygen species
SOD2	superoxide dismutase 2

References

[1]. Varela-Nieto I, Murillo-Cuesta S, Calvino M, Cediel R, Lassaletta L, Drug development for noise-induced hearing loss, Expert Opin. Drug Discov. 15 (12) (2020) 1457–1471. [PubMed: 32838572]

[2]. Hudspeth AJ, Integrating the active process of hair cells with cochlear function, Nat. Rev. Neurosci 15 (9) (2014) 600–614. [PubMed: 25096182]

[3]. Sha SH, Schacht J, Emerging therapeutic interventions against noise-induced hearing loss, Expert Opin. Investig. Drugs 26 (1) (2017) 85–96, 5527323.

[4]. Wagner EL, Shin JB, Mechanisms of hair cell damage and repair, Trends Neurosci. 42 (6) (2019) 6556399, 414–24. [PubMed: 30992136]

[5]. Dieter A, Keppeler D, Moser T, Towards the optical cochlear implant: optogenetic approaches for hearing restoration, EMBO Mol. Med 12 (4) (2020) 7136966, e11618. [PubMed: 32227585]

[6]. Takeda H, Dondzillo A, Randall JA, Gubbels SP, Challenges in cell-based therapies for the treatment of hearing loss, Trends Neurosci. 41 (11) (2018) 823–837. [PubMed: 30033182]

[7]. Kil J, Lobarinas E, Spankovich C, Griffiths SK, Antonelli PJ, Lynch ED, et al. , Safety and efficacy of ebselen for the prevention of noise-induced hearing loss: a randomised, double-blind, placebo-controlled, phase 2 trial, Lancet 390 (10098) (2017) 969–979. [PubMed: 28716314]

[8]. Le Prell CG, Fulbright A, Spankovich C, Griffiths SK, Lobarinas E, Campbell KC, et al. , Dietary supplement comprised of beta-carotene, vitamin C, vitamin E, and magnesium: failure to prevent music-induced temporary threshold shift, Audiol. Neurotol. Extra 6 (2) (2016) 20–39. [PubMed: 27990155]

[9]. Mao H, Chen Y, Noise-induced hearing loss: updates on molecular targets and potential interventions, Neural Plast. 2021 (4784385) (2021) 8279877.

[10]. Ma Y, Wise AK, Shepherd RK, Richardson RT, New molecular therapies for the treatment of hearing loss, Pharmacol. Ther 200 (190–209) (2019) 6626560.

[11]. Nyberg S, Abbott NJ, Shi X, Steyger PS, Dabdoub A, Delivery of therapeutics to the inner ear: the challenge of the blood-labyrinth barrier, Sci. Transl. Med 11 (482) (2019).

[12]. Fetoni AR, Paciello F, Rolesi R, Paludetti G, Troiani D, Targeting dysregulation of redox homeostasis in noise-induced hearing loss: oxidative stress and ROS signaling, Free Radic. Biol. Med 135 (2019) 46–59. [PubMed: 30802489]

[13]. Fujimoto C, Yamasoba T, Mitochondria-targeted antioxidants for treatment of hearing loss: a systematic review, Antioxidants 8 (4) (2019) 6523236.

[14]. Wu F, Hill K, Fang Q, He Z, Zheng H, Wang X, et al. , Traumatic-noise-induced hair cell death and hearing loss is mediated by activation of CaMKKbeta, Cell. Mol. Life Sci.: CMLS 79 (5) (2022) 249. [PubMed: 35438341]

[15]. Wu F, Xiong H, Sha S, Noise-induced loss of sensory hair cells is mediated by ROS/AMPKalpha pathway, Redox Biol. 29 (101406) (2020) 6933152.

[16]. Hill K, Yuan H, Wang X, Sha SH, Noise-induced loss of hair cells and cochlear synaptopathy are mediated by the activation of AMPK, J. Neurosci.: Off. J. Soc. Neurosci 36 (28) (2016) 7497–7510, 4945669.

[17]. Liu F, Zhang Z, Csanady L, Gadsby DC, Chen J, Molecular structure of the human CFTR ion channel, Cell 169 (1) (2017) 85–95, e8. [PubMed: 28340353]

[18]. Elborn JS, Cystic fibrosis, Lancet 388 (10059) (2016) 2519–2531. [PubMed: 27140670]

[19]. Vanherle L, Matthes F, Uhl FE, Meissner A, Ivacaftor therapy post myocardial infarction augments systemic inflammation and evokes contrasting effects with respect to tissue inflammation in brain and lung, Biomed. Pharmacother. = Biomed. Pharmacother 162 (2023), 114628. [PubMed: 37018991]

[20]. Bose SJ, Bijvelds MJC, Wang Y, Liu J, Cai Z, Bot AGM, et al. , Differential thermostability and response to cystic fibrosis transmembrane conductance regulator potentiators of human and mouse F508del-CFTR, Am. J. Physiol. Lung Cell Mol. Physiol 317 (1) (2019). L71–l86. [PubMed: 30969810]

[21]. Borcherding DC, Siefert ME, Lin S, Brewington J, Sadek H, Clancy JP, et al. , Clinically-approved CFTR modulators rescue Nrf2 dysfunction in cystic fibrosis airway epithelia, J. Clin. Invest 129 (8) (2019) 3448–3463. [PubMed: 31145101]

[22]. Ross D, Siegel D, The diverse functionality of NQO1 and its roles in redox control, Redox Biol. 41 (101950) (2021) 8027776.

[23]. Ma CS, Lv QM, Zhang KR, Tang YB, Zhang YF, Shen Y, et al. , NRF2-GPX4/SOD2 axis imparts resistance to EGFR-tyrosine kinase inhibitors in non-small-cell lung cancer cells, Acta Pharmacol. Sin 42 (4) (2021), 613–23, 8115089. [PubMed: 32704041]

[24]. Ryter SW, Heme oxgenase-1, a cardinal modulator of regulated cell death and inflammation, Cells 10 (3) (2021) 7997353.

[25]. Homma K, Miller KK, Anderson CT, Sengupta S, Du GG, Aguinaga S, et al. , Interaction between CFTR and prestin (SLC26A5), Biochim. Biophys. Acta 1798 (6) (2010) 1029–1040, 2862844. [PubMed: 20138822]

[26]. Kongsuphol P, Cassidy D, Hieke B, Treharne KJ, Schreiber R, Mehta A, et al. , Mechanistic insight into control of CFTR by AMPK, J. Biol. Chem 284 (9) (2009) 5645–5653. [PubMed: 19095655]

[27]. Ho MK, Li X, Wang J, Ohmen JD, Friedman RA, FVB/NJ mice demonstrate a youthful sensitivity to noise-induced hearing loss and provide a useful genetic model for the study of neural hearing loss, Audiol Neurotol Extra 4 (1) (2014) 1–11, 3972069. [PubMed: 24707282]

[28]. Fohner AE, McDonagh EM, Clancy JP, Whirl Carrillo M, Altman RB, Klein TE, PharmGKB summary: ivacaftor pathway, pharmacokinetics/pharmacodynamics, Pharmacogenet. Genom. 27 (1) (2017) 39–42.

[29]. (a)Van Goor F, Hadida S, Grootenhuis PD, Burton B, Cao D, Neuberger T, et al. , Rescue of CF airway epithelial cell function in vitro by a CFTR potentiator, VX-770, Proc. Natl. Acad. Sci. USA 106 (44) (2009) 18825–18830, 2773991; [PubMed: 19846789] (b)A.S., J.J, A.H., J.Z, J.M., V.A, C.D., J.Y, C.Y., E.R.O, and P.N are employees of Vertex Pharmaceuticals Incorporated, which is evaluating VX-770 as a potential treatment for cystic fibrosis.

[30]. Hadida S, Van Goor F, Zhou J, Arumugam V, McCartney J, Hazlewood A, et al. , Discovery of N-(2,4-di-tert-butyl-5-hydroxyphenyl)-4-oxo-1,4-dihydroquinoline-3-carboxamide (VX-770, ivacaftor), a potent and orally bioavailable CFTR potentiator, J. Med. Chem 57 (23) (2014) 9776–9795. [PubMed: 25441013]

[31]. Xiong H, Ou Y, Xu Y, Huang Q, Pang J, Lai L, et al. , Resveratrol promotes recovery of hearing following intense noise exposure by enhancing cochlear SIRT1 activity, Audiol. Neuro-Otol 22 (4–5) (2017) 303–310.

[32]. Fang QJ, Wu F, Chai R, Sha SH, Cochlear surface preparation in the adult mouse, J. Vis. Exp.: JoVE 153 (2019) 7217453.

[33]. Viberg A, Canlon B, The guide to plotting a cochleogram, Hear. Res 197 (1–2) (2004) 1–10. [PubMed: 15504598]

[34]. Chen FQ, Schacht J, Sha SH, Aminoglycoside-induced histone deacetylation and hair cell death in the mouse cochlea, J. Neurochem 108 (5) (2009) 1226–1236, 3341988. [PubMed: 19141081]

[35]. Park C, Thein P, Kalinec G, Kalinec F, HEI-OC1 cells as a model for investigating prestin function, Hear. Res 335 (2016) 9–17. [PubMed: 26854618]

[36]. Rieger AM, Nelson KL, Konowalchuk JD, Barreda DR, Modified annexin V/propidium iodide apoptosis assay for accurate assessment of cell death, J. Vis. Exp (50) (2011).

[37]. Aranda A, Sequedo L, Tolosa L, Quintas G, Burello E, Castell JV, et al. , Dichloro-dihydro-fluorescein diacetate (DCFH-DA) assay: a quantitative method for oxidative stress assessment of nanoparticle-treated cells, Toxicol. Vitr 27 (2) (2013) 954–963.

[38]. Taylor-Cousar JL, Munck A, McKone EF, van der Ent CK, Moeller A, Simard C, et al. , Tezacaftor-ivacaftor in patients with cystic fibrosis homozygous for Phe508del, N. Engl. J. Med 377 (21) (2017) 2013–2023. [PubMed: 29099344]

[39]. Dang R, Wang M, Li X, Wang H, Liu L, Wu Q, et al. , Edaravone ameliorates depressive and anxiety-like behaviors via Sirt1/Nrf2/HO-1/Gpx4 pathway, J. Neuroinflamm. 19 (1) (2022) 41.

[40]. Qiu YB, Wan BB, Liu G, Wu YX, Chen D, Lu MD, et al. , Nrf2 protects against seawater drowning-induced acute lung injury via inhibiting ferroptosis, Respir. Res 21 (1) (2020) 232. [PubMed: 32907551]

[41]. King JD Jr., Fitch AC, Lee JK, McCane JE, Mak DO, Foskett JK, et al. , AMP-activated protein kinase phosphorylation of the R domain inhibits PKA stimulation of CFTR, Am. J. Physiol. Cell Physiol. 297 (1) (2009) C94–C101. [PubMed: 19419994]

[42]. Liu C, Tang D, Zheng Z, Lu X, Li W, Zhao L, et al. , A PRMT5 inhibitor protects against noise-induced hearing loss by alleviating ROS accumulation, Ecotoxicol. Environ. Saf 243 (2022), 113992. [PubMed: 35994911]

[43]. Rousset F, Nacher-Soler G, Kokje VBC, Sgroi S, Coelho M, Krause KH, et al. , NADPH oxidase 3 deficiency protects from noise-induced sensorineural hearing loss, Front. Cell Dev. Biol 10 (2022), 832314. [PubMed: 35273964]

[44]. Zhang Y, Li Q, Han C, Geng F, Zhang S, Qu Y, et al. , Superoxide dismutase@ zeolite imidazolate framework-8 attenuates noise-induced hearing loss in rats, Front. Pharmacol 13 (2022), 885113. [PubMed: 35662706]

[45]. Park JS, Jou I, Park SM, Attenuation of noise-induced hearing loss using methylene blue, Cell Death Dis. 5 (4) (2014), e1200. [PubMed: 24763057]

[46]. Fransson AE, Videhult Pierre P, Risling M, Laurell GFE, Inhalation of molecular hydrogen, a rescue treatment for noise-induced hearing loss, Front. Cell Neurosci. 15 (2021), 658662. [PubMed: 34140880]

[47]. de Bari L, Favia M, Bobba A, Lassandro R, Guerra L, Atlante A, Aberrant GSH reductase and NOX activities concur with defective CFTR to pro-oxidative imbalance in cystic fibrosis airways, J. Bioenerg. Biomembr. 50 (2) (2018) 117–129. [PubMed: 29524019]

[48]. Fetoni AR, Paciello F, Rolesi R, Eramo SL, Mancuso C, Troiani D, et al. , Rosmarinic acid up-regulates the noise-activated Nrf2/HO-1 pathway and protects against noise-induced injury in rat cochlea, Free Radic. Biol. Med 85 (2015) 269–281. [PubMed: 25936352]

[49]. He ZH, Pan S, Zheng HW, Fang QJ, Hill K, Sha SH, Treatment with calcineurin inhibitor FK506 attenuates noise-induced hearing loss, Front. Cell Dev. Biol 9 (2021), 648461. [PubMed: 33777956]

[50]. Yuan H, Wang X, Hill K, Chen J, Lemasters J, Yang SM, et al. , Autophagy attenuates noise-induced hearing loss by reducing oxidative stress, Antioxid. Redox Signal. 22 (15) (2015) 1308–1324. [PubMed: 25694169]

[51]. Kelly M, Trudel S, Brouillard F, Bouillaud F, Colas J, Nguyen-Khoa T, et al. , Cystic fibrosis transmembrane regulator inhibitors CFTR(inh)-172 and GlyH-101 target mitochondrial functions, independently of chloride channel inhibition, J. Pharmacol. Exp. Ther 333 (1) (2010) 60–69. [PubMed: 20051483]

[52]. Honkura Y, Matsuo H, Murakami S, Sakiyama M, Mizutari K, Shiotani A, et al. , NRF2 is a key target for prevention of noise-induced hearing loss by reducing oxidative damage of cochlea, Sci. Rep 6 (2016) 19329. [PubMed: 26776972]

[53]. Zeng J-W, Zeng X-L, Li F-Y, Ma M-M, Yuan F, Liu J, et al. , Cystic Fibrosis Transmembrane Conductance Regulator (CFTR) prevents apoptosis induced by hydrogen peroxide in basilar artery smooth muscle cells, Apoptosis 19 (9) (2014) 1317–1329. [PubMed: 24999019]

[54]. Kalinec GM, Webster P, Lim DJ, Kalinec F, A cochlear cell line as an in vitro system for drug ototoxicity screening, Audiol. Neuro-Otol. 8 (4) (2003) 177–189.

[55]. Jat PS, Noble MD, Ataliotis P, Tanaka Y, Yannoutsos N, Larsen L, et al. , Direct derivation of conditionally immortal cell lines from an H-2Kb-tsA58 transgenic mouse, Proc. Natl. Acad. Sci. USA 88 (12) (1991) 5096–5100. [PubMed: 1711218]

[56]. Chen FQ, Hill K, Guan YJ, Schacht J, Sha SH, Activation of apoptotic pathways in the absence of cell death in an inner-ear immortomouse cell line, Hear. Res 284 (1–2) (2012) 33–41. [PubMed: 22240458]

[57]. Xu B, Qin Y, Li D, Cai N, Wu J, Jiang L, et al. , Inhibition of PDE4 protects neurons against oxygen-glucose deprivation-induced endoplasmic reticulum stress through activation of the Nrf-2/HO-1 pathway, Redox Biol. 28 (2020), 101342. [PubMed: 31639651]

[58]. Singh A, Venkannagari S, Oh KH, Zhang YQ, Rohde JM, Liu L, et al. , Small molecule inhibitor of NRF2 selectively intervenes therapeutic resistance in KEAP1-deficient NSCLC tumors, ACS Chem. Biol 11 (11) (2016) 3214–3225. [PubMed: 27552339]

[59]. Lin Y, Luo T, Weng A, Huang X, Yao Y, Fu Z, et al. , Gallic acid alleviates gouty arthritis by inhibiting NLRP3 inflammasome activation and pyroptosis through enhancing Nrf2 signaling, Front. Immunol 11 (2020), 580593. [PubMed: 33365024]

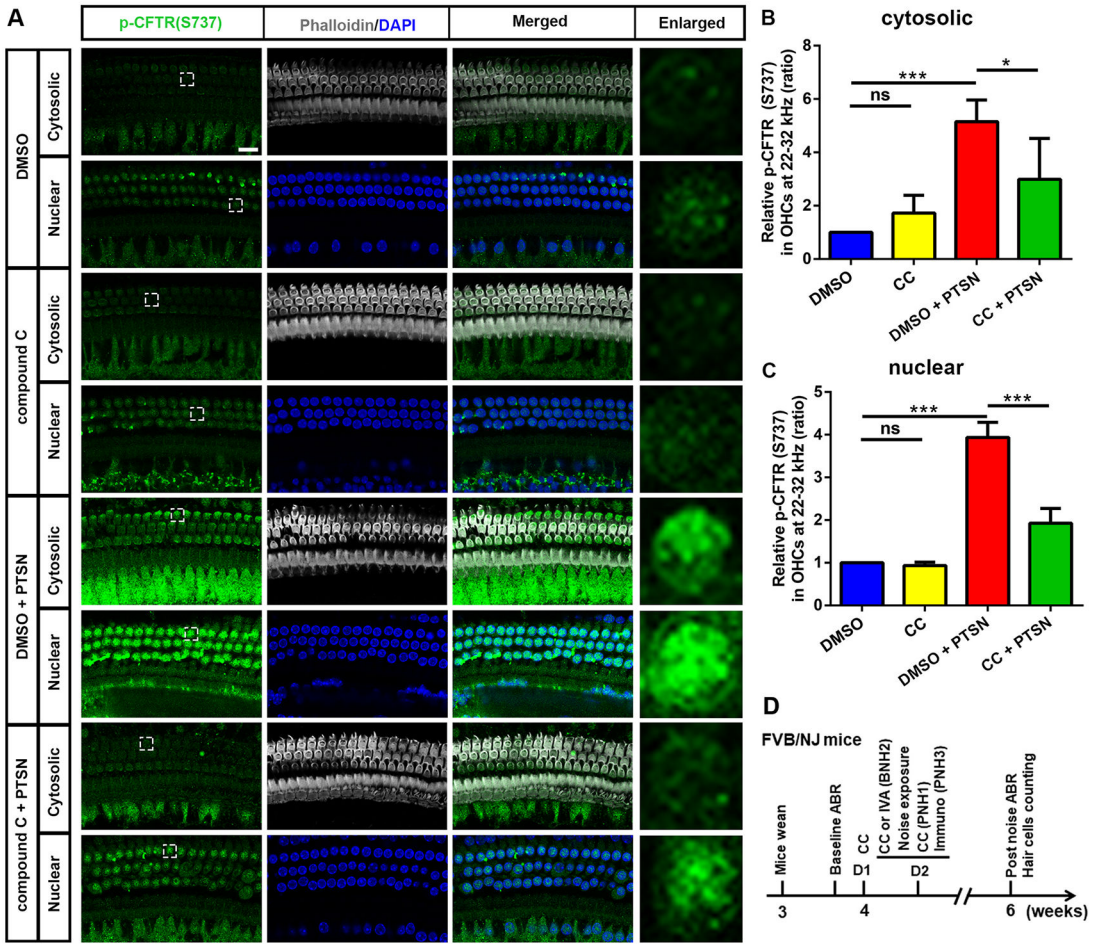

Fig. 1.

Treatment with AMPKα inhibitor compound C prevents noise-increased phosphorylation of CFTR (S737) in OHCs. (A) Representative images show that treatment with compound C (CC) prevents noise-increased immunolabeling for p-CFTR (S737) in both the cytosol and nuclei of OHCs. The enlarged images of the OHCs allow for better visualization of punctate immunolabeling. Compound C alone shows p-CFTR (S737) labeling intensity similar to solvent controls (DMSO). Phalloidin (white) and DAPI (blue) were used as counterstaining for visualization of OHC structure and nuclei. PTSN: permanent threshold shift noise; Scale bar = 10 μm. (B–C) Semi-quantification of immunolabeling for p-CFTR (S737) in the cytosol (B) and nuclei (C) of OHCs confirms a significant increase 3 h after noise exposure, while treatment with compound C prevents such effects. Data are presented as means + SD, $n = 3$ mice in each group. One cochlea was used per mouse, ns: non-significant, *$p < 0.05$, ***$p < 0.001$. (D) Timeline of the in-vivo experiments: FVB/NJ mice were weaned at 21 days (3 weeks) and had baseline ABRs at 25 days. At the age of 4 weeks, one day before noise exposure (D1), mice received the first dose of compound C (CC). On day 2 (D2), mice received a second dose of CC 2 h before noise exposure, followed by noise exposure for 2 h. Mice received a third dose of CC 1 h after noise exposure. For experiments using ivacaftor, mice only received one dose of ivacaftor 2 h before noise exposure. Some mice were euthanized 3 h after the exposure for immunolabeling and others had final ABR

measurements 2 weeks after the noise exposure (at the age of 6 weeks) and were euthanized for surface preparations for hair cell counts.

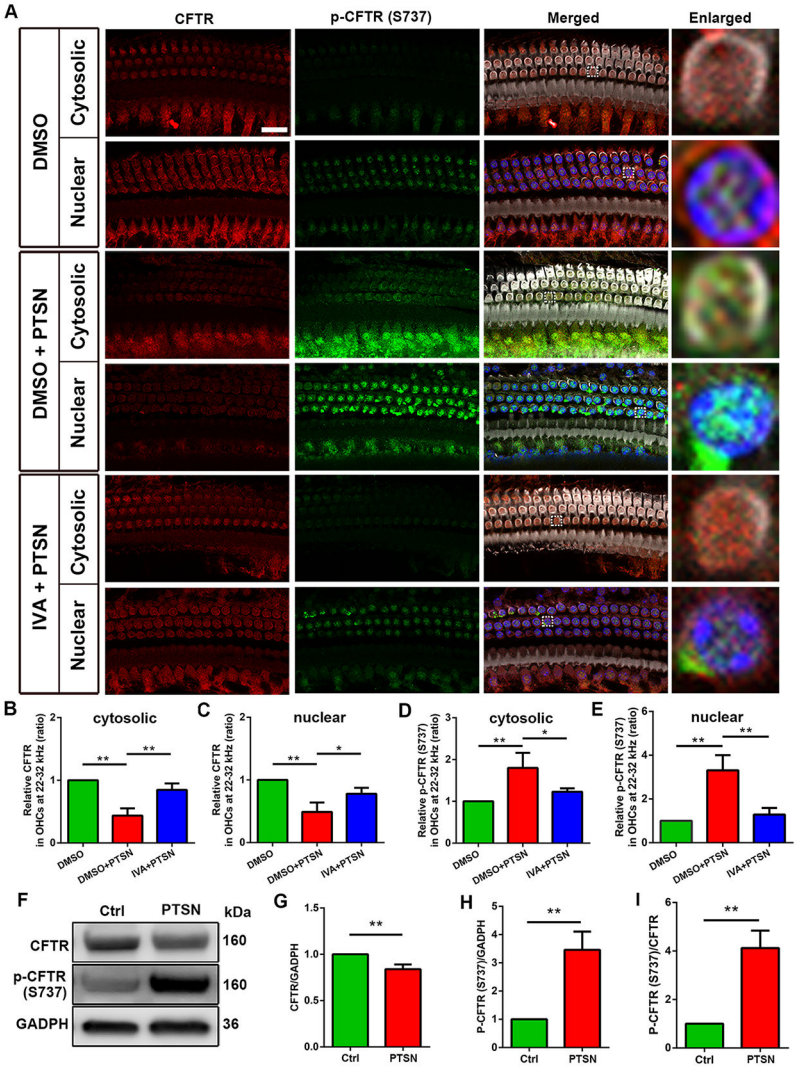

Fig. 2.

Treatment with ivacaftor prevents the decrease of CFTR and the increase of p-CFTR (S737) after noise exposure in OHCs. (A) Representative images show immunolabeling for CFTR (red) and p-CFTR (S737, green) in OHC cytosol and nuclei in the upper basal turn measured 3 h after noise exposure. The enlarged OHCs allow for better visualization of the punctate labeling for CFTR and p-CFTR (S373). These images are representative of 3 mice in each group. Phalloidin (white) and DAPI (blue) were used as counterstaining for visualization of OHC cytoskeletal structure and nuclei, respectively. DMSO (control, solvent of ivacaftor); IVA (ivacaftor). Scale bar = 10 μm. (B–E) Semi-quantification of immunolabeling in grayscale of CFTR and p-CFTR (S737) in the OHC cytosol and nuclei shows that treatment with ivacaftor significantly prevents noise-decreased CFTR and increased p-CFTR (S737). Data are presented as means + SD, $n = 3$, $*p < 0.05$, $**p < 0.01$. (F) Representative immunoblots reveal a decrease in total CFTR expression and increase in p-CFTR (S737) in whole cochlear homogenates 3 h after noise exposure. These blots are representative of 3 repetitions with two cochleae per sample. GADPH serves as loading control. (G–I) Quantification of CFTR and p-CFTR (S737) band densities shows a significant decrease

in CFTR levels (G), an increase in p-CFTR (S737) levels (H), and an increase in the ratio of p-CFTR (S737) to CFTR (I) in the PTS noise group compared to controls. Data are presented as means + SD, $n = 3$, $^{**}p < 0.01$.

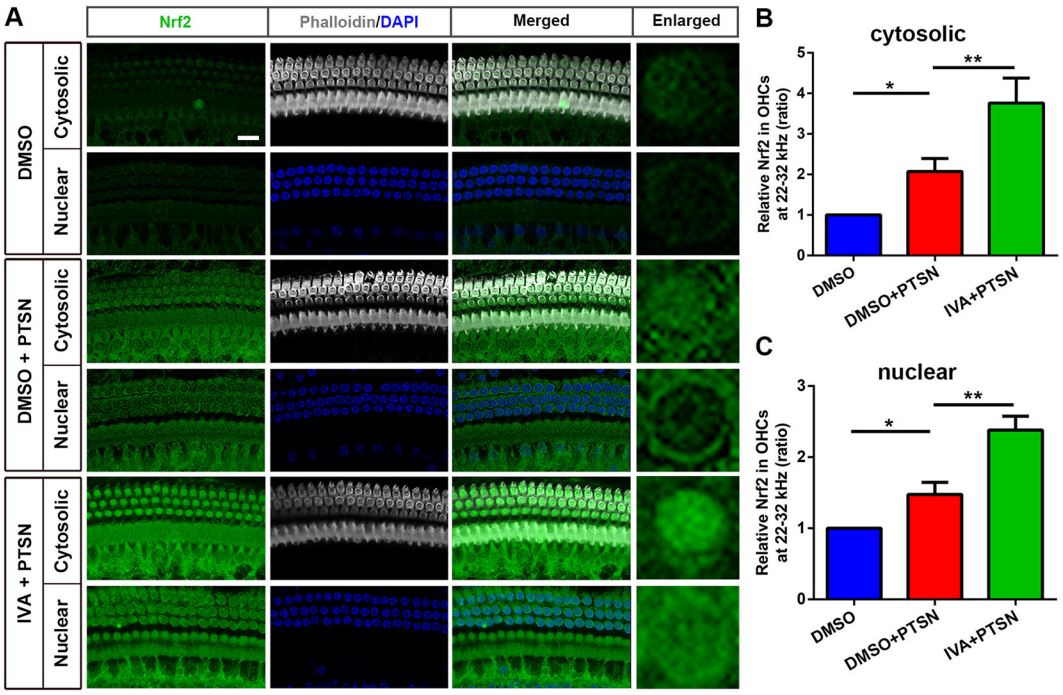

Fig. 3.

Treatment with ivacaftor increases Nrf2 expression in OHCs. (A) Representative images show that Nrf2 (green) in OHCs mildly increases in both the cytosol and nuclei 3 h after noise exposure in the presence of DMSO, whereas ivacaftor pretreatment strongly increases Nrf2 immunolabeling. Phalloidin (white) and DAPI (blue) were used as counterstaining for visualization of OHCs. Scale bar = 10 μm. (B–C) Semi-quantitative analysis of immunolabeling in grayscale of Nrf2 in the OHC cytosol (B) and nuclei (C) confirms a mild increase with DMSO and 2-fold increase with ivacaftor 3 h after noise exposure. All bar graph data are presented as means + SD, $n = 3$ in each group. One cochlea was used per mouse, ns: non-significant, *$p < 0.05$, **$p < 0.01$.

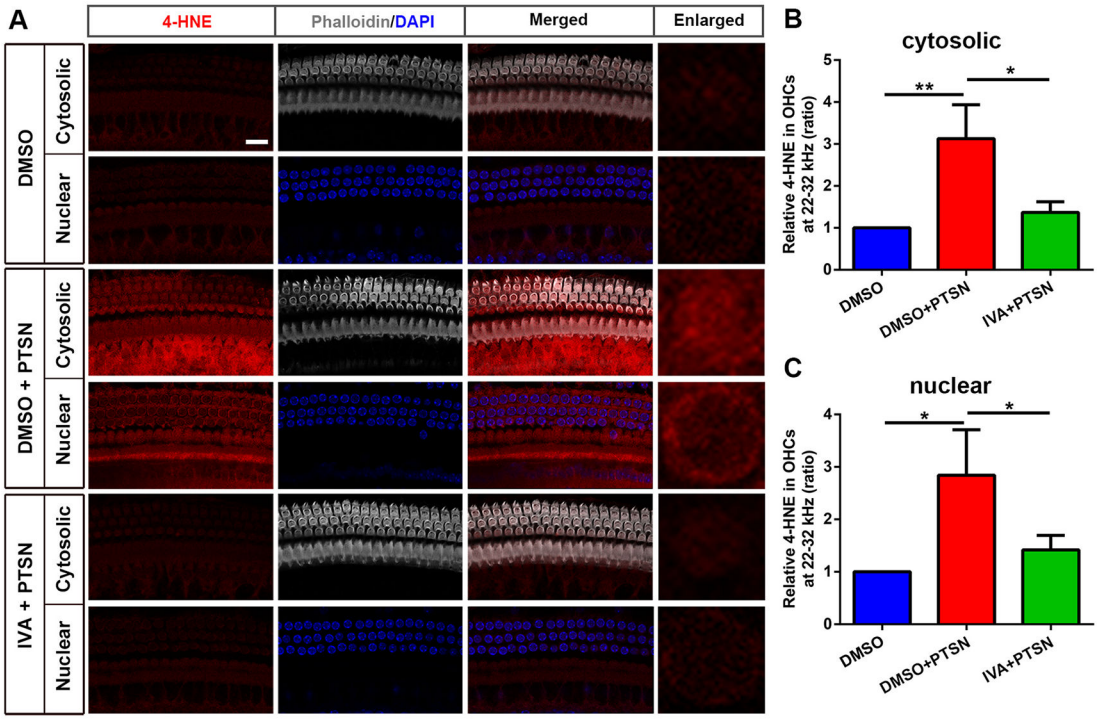

Fig. 4.

Treatment with ivacaftor reduces noise-enhanced formation of 4-HNE in OHCs. (A) Immunolabeling for 4-HNE (4-hydroxynonenal) in both the cytosol and nuclei of OHCs shows an increase 3 h after exposure to noise and this increase is abolished by ivacaftor pretreatment. Scale bar = 10 μm. (B–C) Semi-quantitative analysis of 4-HNE in the OHC cytosol (F) and nuclei (G) confirms a significant increase 3 h after noise exposure. This effect is blocked by ivacaftor treatment. All data in the bar graphs are presented as means + SD, $n = 3$ in each group, ns: non-significant, *$p < 0.05$, **$p < 0.01$.

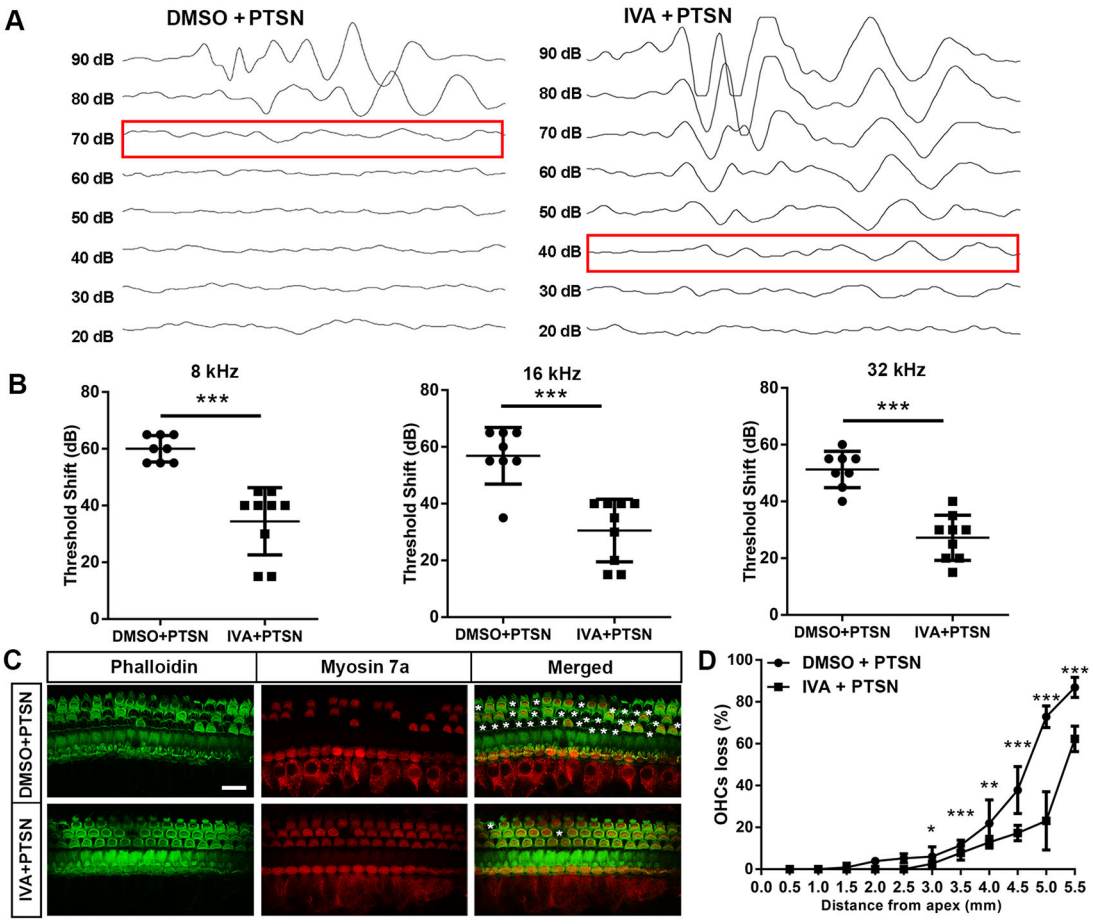

Fig. 5.

Treatment with ivacaftor attenuates noise-induced hair cell loss and auditory threshold shifts in vivo. ABR waveforms at 32 kHz show auditory thresholds at 70 dB SPL in noise-exposed mice and at 40 dB SPL in noise-exposed mice pre-treated with ivacaftor when measured 14 d after the PTS-causing exposure. DMSO: vehicle control, IVA: ivacaftor. Treatment with ivacaftor prevents noise-induced auditory threshold shifts at all tested frequencies (8, 16, and 32 kHz). Data are presented as individual points with means ± SD, ***$p < 0.001$. (C) Representative images (taken 5 mm from the apex of the cochlear spiral) display phalloidin- (green) and myosin-7a- (red) labeled sensory hair cells in DMSO + noise and ivacaftor + noise groups 14 d after noise exposure. Missing OHCs are marked with stars. Scale bar = 10 μm. (D) Hair cells were counted along the entire length of the cochlear spiral. Treatment with ivacaftor reduces noise-induced OHC loss. Data are presented as means ± SD, $n = 5$ in the DMSO + noise group, $n = 4$ in the IVA + noise group. One cochlea was used per mouse. *$p < 0.05$, **$p < 0.01$, ***$p < 0.001$.

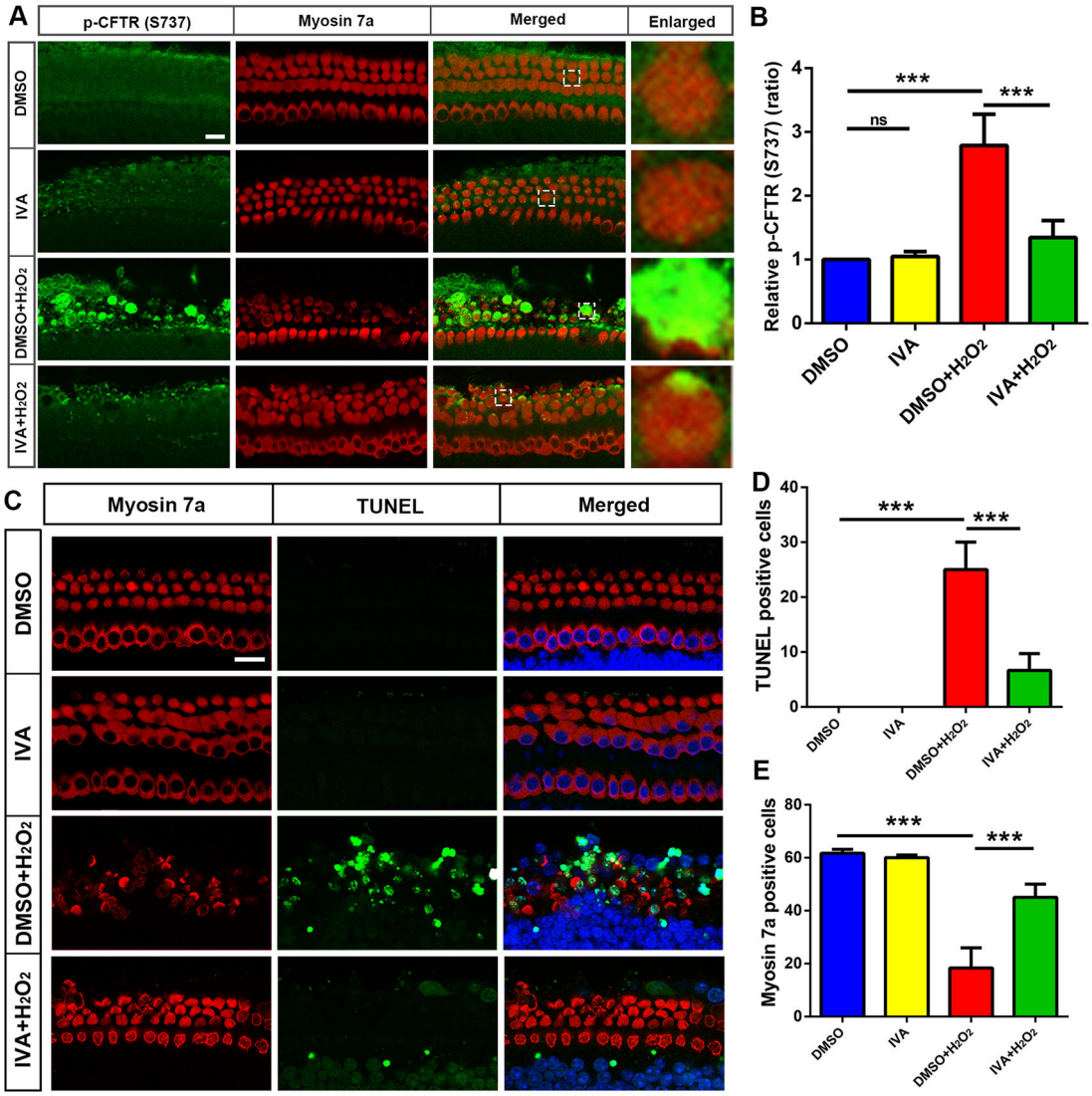

Fig. 6.

Increased p-CFTR (S737) and OHC death in organotypic explants after hydrogen peroxide treatment are diminished by application of ivacaftor. (A) Images of cochlear organotypic explant cultures (p3 mice) reveal strong p-CFTR (S737, green) immunolabeling in OHCs after hydrogen peroxide exposure for 30 min (panel: DMSO + H_2O_2). Additional treatment with ivacaftor reduces the hydrogen-peroxide-enhanced p-CFTR (S737) in OHCs (panel: IVA + H_2O_2). There are no obvious changes in p-CFTR (S737) labeling in the DMSO or IVA-only groups without exposure to hydrogen peroxide (panel: DMSO or IVA). Red: myosin-7a-labeled hair cells, IVA: ivacaftor. Scale bar = 10 μm. (B) Semi-quantification of the p-CFTR (S737) labeling in grayscale in OHCs confirms a significant increase after hydrogen peroxide exposure. This effect is attenuated by pretreatment with ivacaftor. (C) TUNEL staining shows hydrogen-peroxide-induced apoptotic cell death (green). Red: myosin-7a-labeled hair cells. Scale bar = 10 μm. (D–E) Counts of TUNEL-positive cells (D) and myosin-7a-positive cells (E) show a significant increase in TUNEL-positive cells accompanied by a reduction in myosin-7a-positive cells after hydrogen peroxide exposure.

Pretreatment with ivacaftor significantly diminishes such effects. All data in the bar graphs are presented as means + SD, $n = 3$ in each group, ns: non-significant, ***$p < 0.001$.

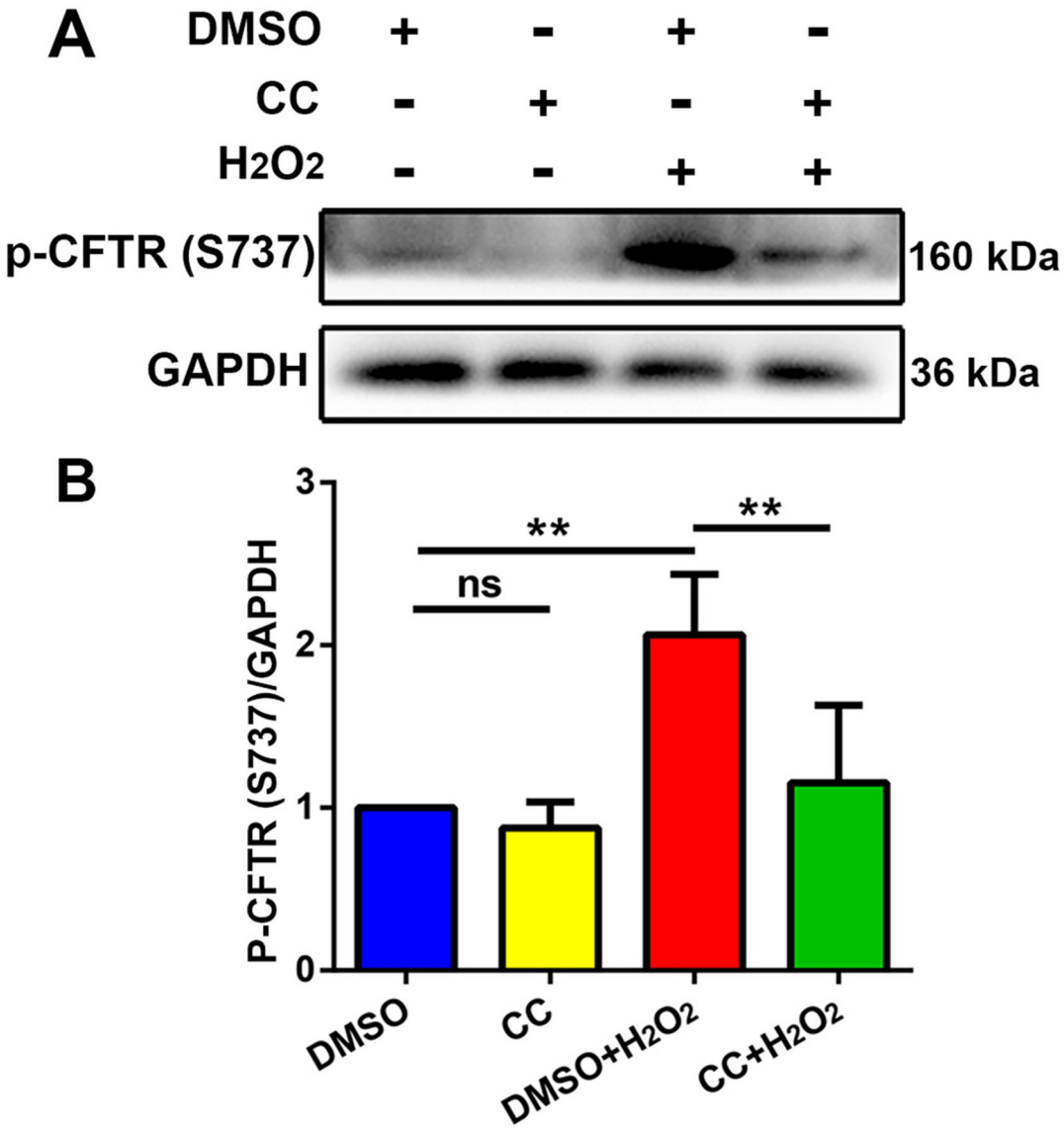

Fig. 7.

Application of compound C diminishes hydrogen-peroxide-increased p-CFTR (S737) expression in HEI-OC1 cells. (A) Representative immunoblots show p-CFTR (S737) expression with or without hydrogen peroxide or compound C treatment versus DMSO alone (vehicle control). HEI-OC1 cells were pretreated with 5 μM compound C or an equal concentration of DMSO for 12 h. The groups were then treated with 10 mM hydrogen peroxide for 15 min. GAPDH serves as the sample loading control. (B) Densitometric analysis of the p-CFTR (S737) band normalized to GAPDH shows that the hydrogen-peroxide-induced increase in p-CFTR (S737) levels is mitigated by compound C pretreatment. Data are presented as the means + SD, $n = 4$ in each group; ns: non-significant, $^{*}p < 0.05$, $^{**}p < 0.01$.

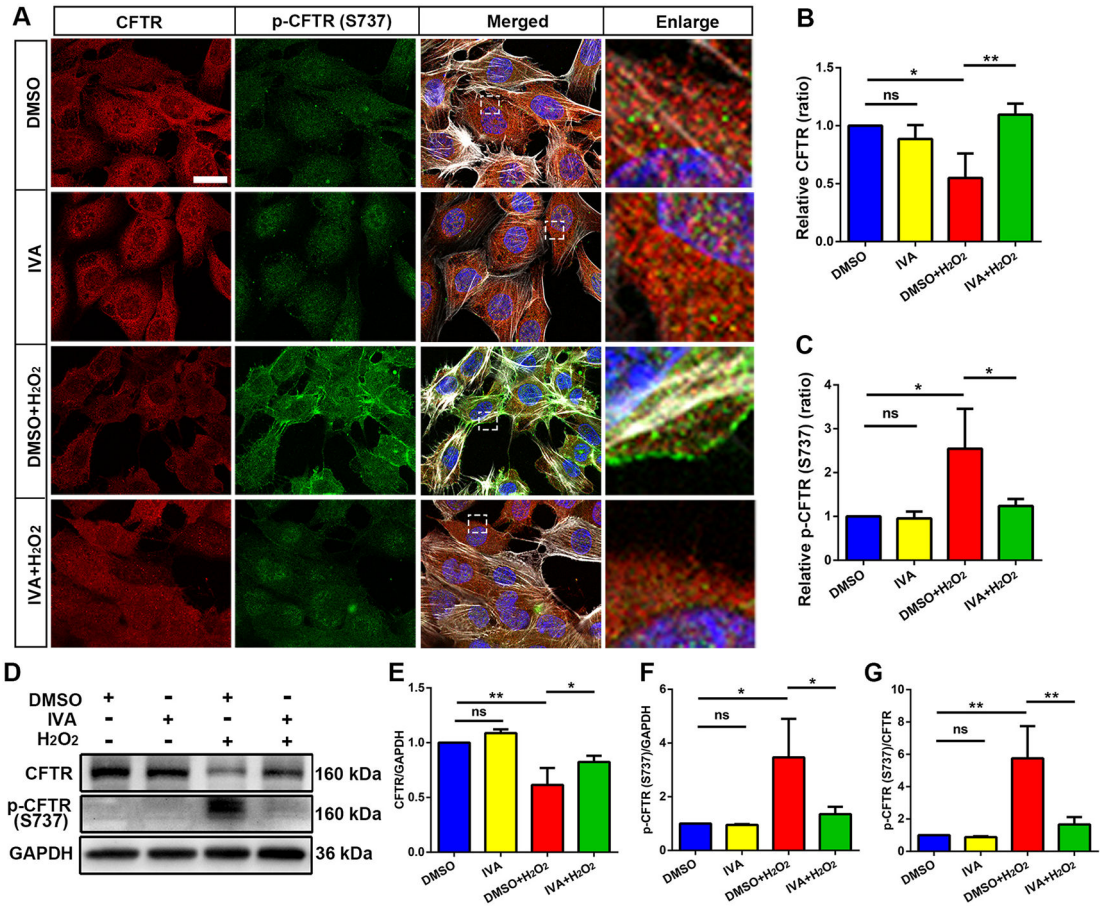

Fig. 8.

Exposure of HEI-OC1 cells to hydrogen peroxide decreases CFTR and increases p-CFTR (S737) expression, while administration of ivacaftor diminishes such effects. (A) Immunolabeling of CFTR (red) and p-CFTR (S737) (green) in HEI-OC1 cells shows a decrease in CFTR and increase in p-CFTR (S737) labeling after exposure to hydrogen peroxide. These changes are attenuated by ivacaftor pretreatment. Phalloidin (white) and DAPI (blue) were used for counterstaining to visualize the cell structure and nuclei. The enlarged HEI-OC1 cells allow for better visualization of the punctate CFTR labeling localized to the cytosol and p-CFTR (S737) localized at the cell membrane. Scale bar = 10 μm. (B–C) Semi-quantification of immunolabeling for CFTR and p-CFTR (S737) confirms a significant decrease in CFTR (B) and an increase in p-CFTR (S737) (C) after hydrogen peroxide exposure, while treatment with ivacaftor prevents these effects. Data are presented as the means + SD, $n = 3$ in each group. ns: non-significant, $*p < 0.05$, $**p < 0.01$. (D) Representative immunoblots show CFTR and p-CFTR (S737) with or without hydrogen peroxide or ivacaftor treatment versus DMSO alone (control). HEI-OC1 cells were pretreated with 5 μM ivacaftor or equal concentration of DMSO for 12 h then treated with or without exposure to 10 mM hydrogen peroxide for 15 min. GAPDH serves as the sample loading control. (E–G) Densitometric analysis of the total CFTR or p-CFTR (S737) bands normalized to GAPDH confirms a significant decrease in CFTR and an increase in p-CFTR (S737) after exposure to hydrogen peroxide. The ratio of p-CFTR (S737) to CFTR also

shows a significant increase (G). These effects are attenuated by ivacaftor pretreatment. Data are presented as the means + SD, $n = 3$ in each group, ns: non-significant, $*p < 0.05$, $**p < 0.01$.

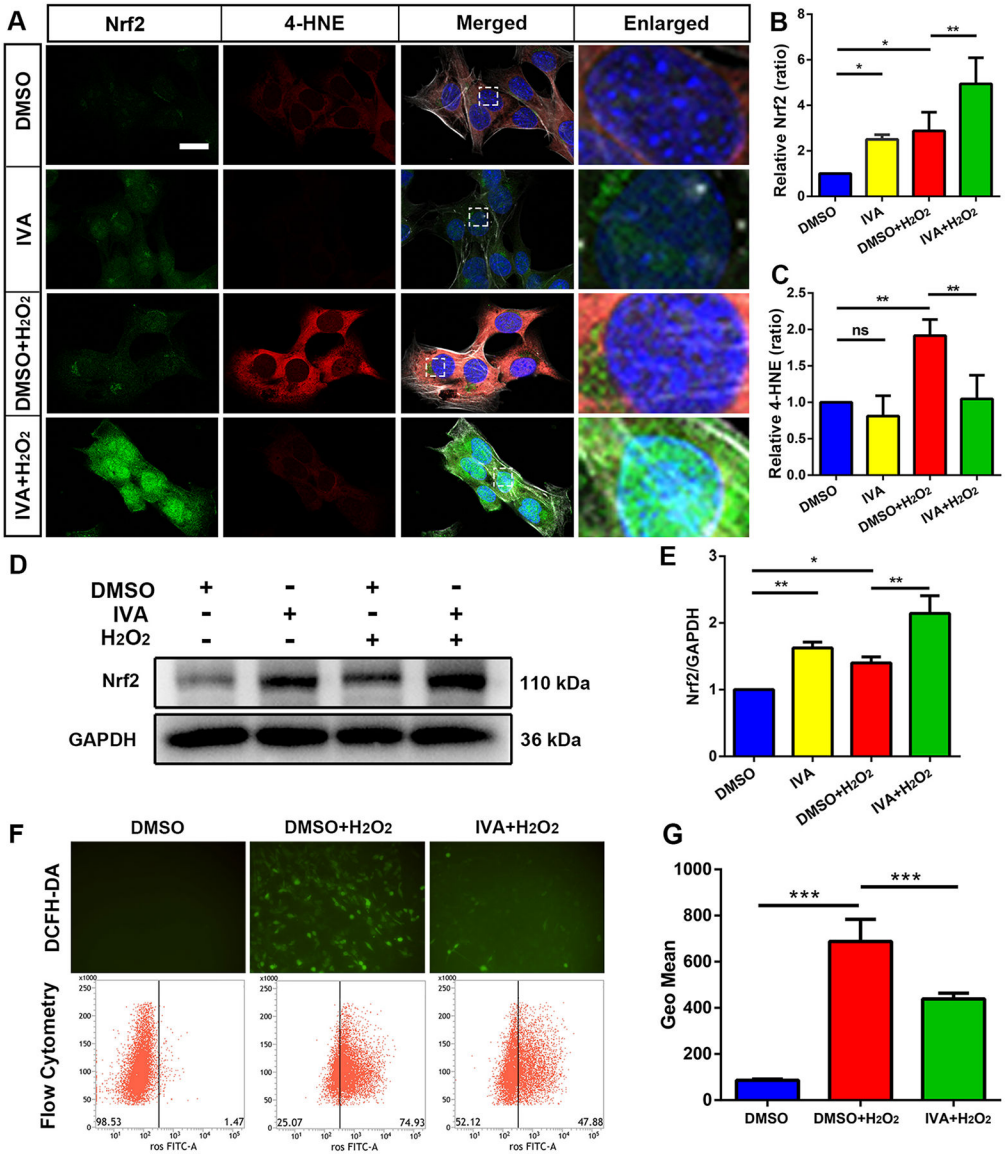

Fig. 9.

Ivacaftor increases Nrf2 expression and reduces 4-HNE accumulation in hydrogen-peroxide-treated HEI-OC1 cells. (A) Representative immunolabeling for 4-HNE (red) and Nrf2 (green) in HEI-OC1 cells show a strong labeling for 4-HNE and a mild increase in Nrf2 after exposure to hydrogen peroxide. Administration of ivacaftor reduces hydrogen-peroxide-increased 4-HNE and further increases Nrf2 labeling. The enlarged HEI-OC1 cells are for better visualization of the labeling. Phalloidin (white) and DAPI (blue) were used for counterstaining to visualize the cell cytoskeletal structure and nuclei. Scale bar = 10 μm. (B–C) Semi-quantification of immunolabeling for Nrf2 and 4-HNE in HEI-OC1 cells. DMSO is used as the solvent for ivacaftor. Application of ivacaftor or DMSO + hydrogen peroxide mildly increases Nrf2, but the amount of Nrf2 after hydrogen peroxide treatment is doubled by pretreatment with ivacaftor (B). Semi-quantification confirms a significant increase in 4-HNE after hydrogen peroxide application, while pretreatment with ivacaftor

mitigates such an increase (C). Data are presented as means + SD, $n = 4$ in each group, ns: non-significant, $*p < 0.05$, $**p < 0.01$. (D–E) Immunoblots show high Nrf2 band densities after ivacaftor alone or hydrogen peroxide administration and even higher band densities after ivacaftor and hydrogen peroxide co-treatment. GAPDH serves as the sample loading control (D). Semi-quantified band densities confirm a significant increase in Nrf2 protein levels (E). Data are presented as means + SD, $n = 3$ in each group, $*p < 0.05$, $**p < 0.01$. (F–G) ROS detection by DCFH-DA flow cytometry shows an increase in ROS accumulation after hydrogen peroxide stimulation of HEI-OC1 cells, while pretreatment with ivacaftor blocks this effect (F). Quantification of ROS levels confirms a significant increase after hydrogen peroxide exposure and decrease after ivacaftor administration (G). Flow cytometry data were averaged over 3–5 independent runs. Data are presented as means + SD, DMSO group: $n = 3$, DMSO + H_2O_2 group: $n = 5$, IVA + H_2O_2 group: $n = 4$, $***p < 0.001$.

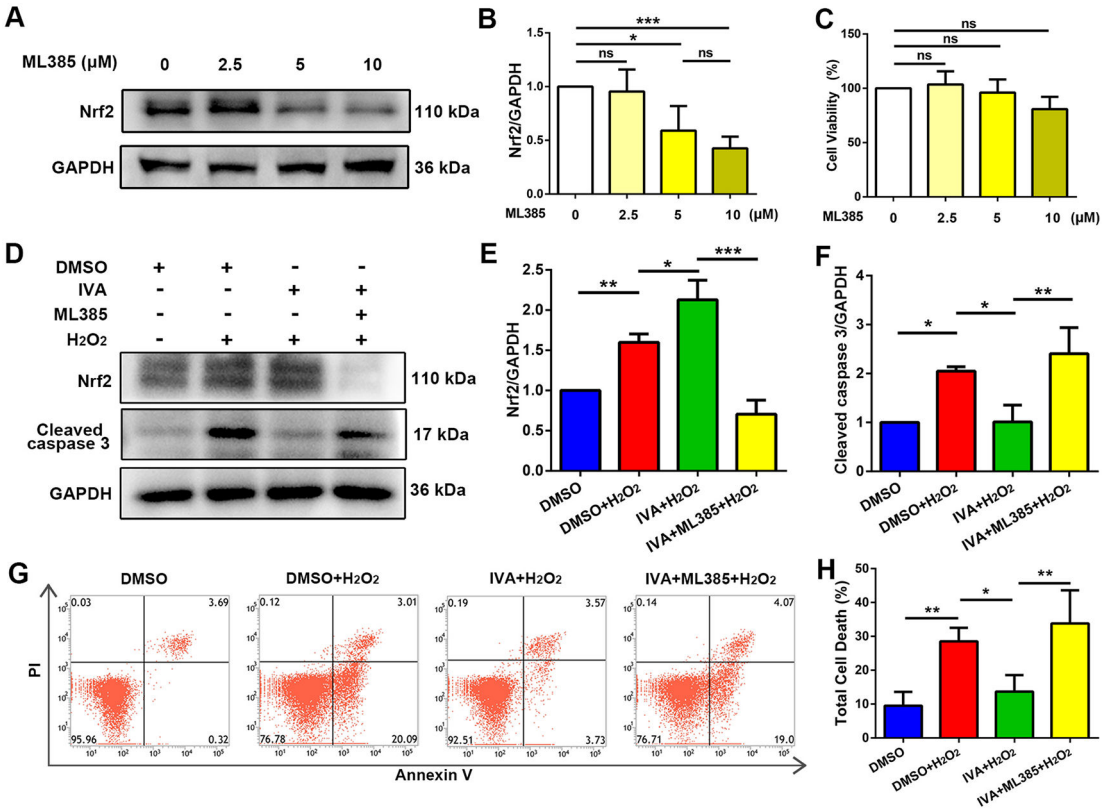

Fig. 10.

Inhibition of Nrf2 by ML385 counteracts the protective effect of ivacaftor in hydrogen-peroxide-treated HEI-OC1 cells. (A–B) Immunoblots show dose-dependent suppression of Nrf2 by ML385 treatment (24 h) in HEI-OC1 cells. GAPDH serves as a loading control (A). Semi-quantitative analysis of Nrf2 protein expression confirms a significant decrease with 5-μM or 10-μM ML385 treatment but not with 2.5-μM treatment (B). (C) Cell viability analysis with the Cell Counting Kit-8 (CCK-8) shows no effect on cell viability at the tested doses of ML385 from 2.5 to 10 μM. (D–F) Immunoblots show that pretreatment with ML385 blocks ivacaftor-increased Nrf2, but the cleaved caspase-3 band remains intense (D). Semi-quantification of Nrf2 and cleaved caspase-3 band densities confirms that ivacaftor-enhanced Nrf2 levels are reversed by pretreatment with 5 μM ML385, (E), while the levels of cleaved caspase 3 remain similar to the hydrogen-peroxide-treated group (F). (G) An annexin V/PI flow cytometry assay shows that the ivacaftor-inhibited, hydrogen-peroxide-induced cell death is reversed by pretreatment with ML385. (H) Quantitative analysis of total cell death in the Annexin V/PI assay shows hydrogen-peroxide-induced cell death is prevented by ivacaftor pretreatment, but such a protective effect is abolished by pretreatment with ML385. Flow cytometry data were averaged over 3 independent runs. Data are presented as the means + SD, $n = 3$, *$p < 0.05$, **$p < 0.01$.

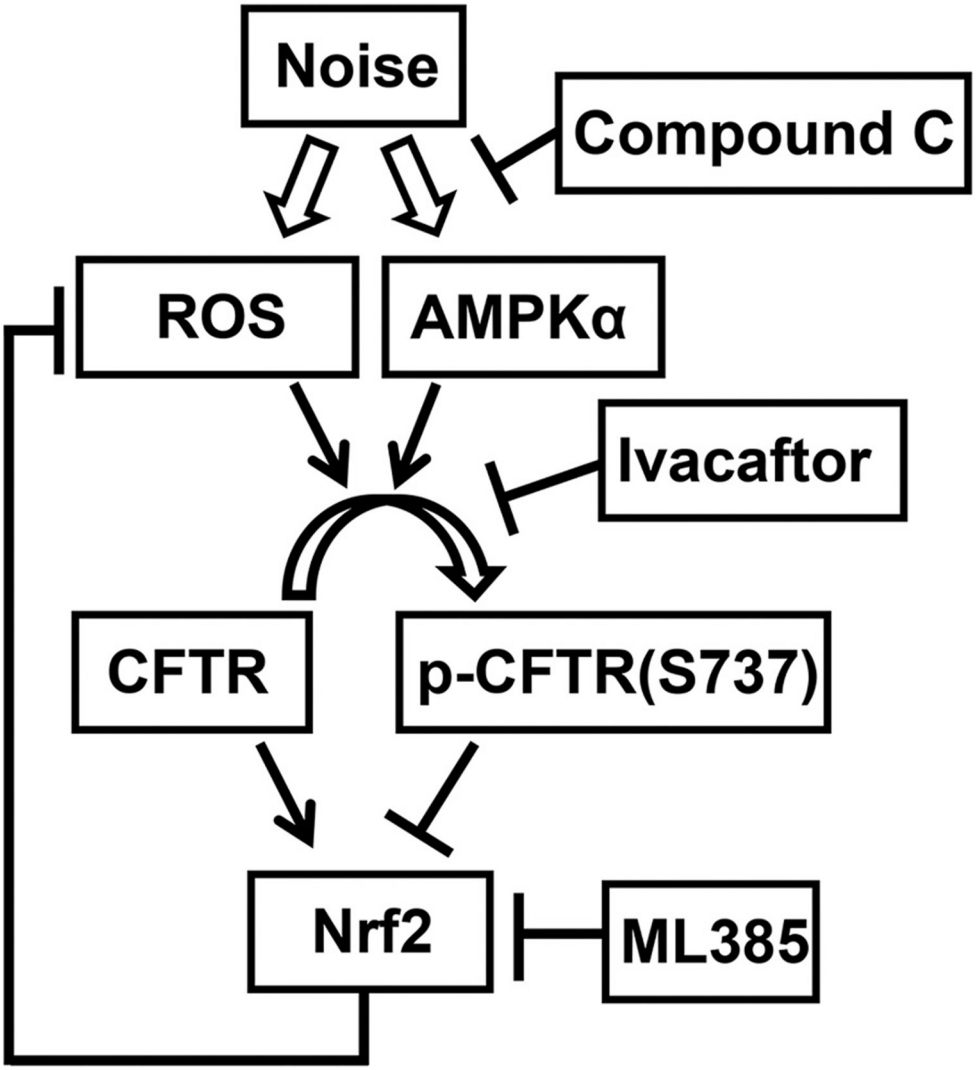

Fig. 11.

A schematic illustration of a working hypothesis in noise-induced hearing loss. Our results from in-vivo and in-vitro experiments suggest that noise exposure activates AMPKα and increases ROS formation. These sequelae in turn inhibit CFTR by increasing p-CFTR (S737) in OHCs. Treatment with ivacaftor diminishes noise-increased p-CFTR (S737) and increases Nrf2 expression, thus protects against noise-induced outer hair cell loss and hearing loss via inhibition of ROS damage. Additionally, our in-vitro data using ML385, a specific Nrf2 inhibitor, further suggest that the protective effects of ivacaftor against oxidative stress involve Nrf2.